IMF

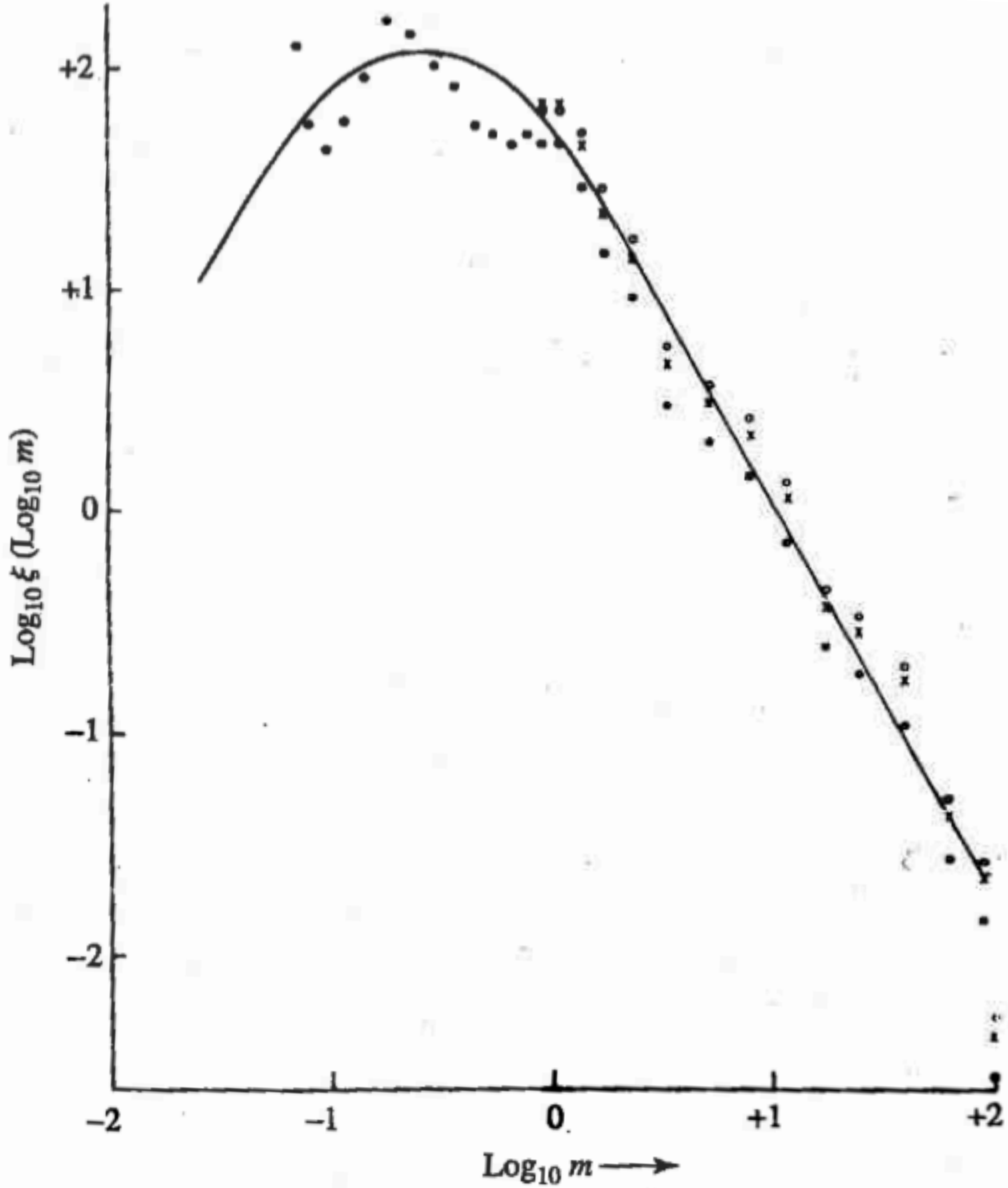

FIGURE 12.12 The initial mass function, ξ, shows the number of stars per unit area of the Milky Way's disk per unit interval of logarithmic mass that is produced in different mass intervals. The individual points represent observational data and the solid line is a theoretical estimate. Masses are in solar units. (Figure adapted from Rana, *Astron. Astrophys.*, *184*, 104, 1987.)

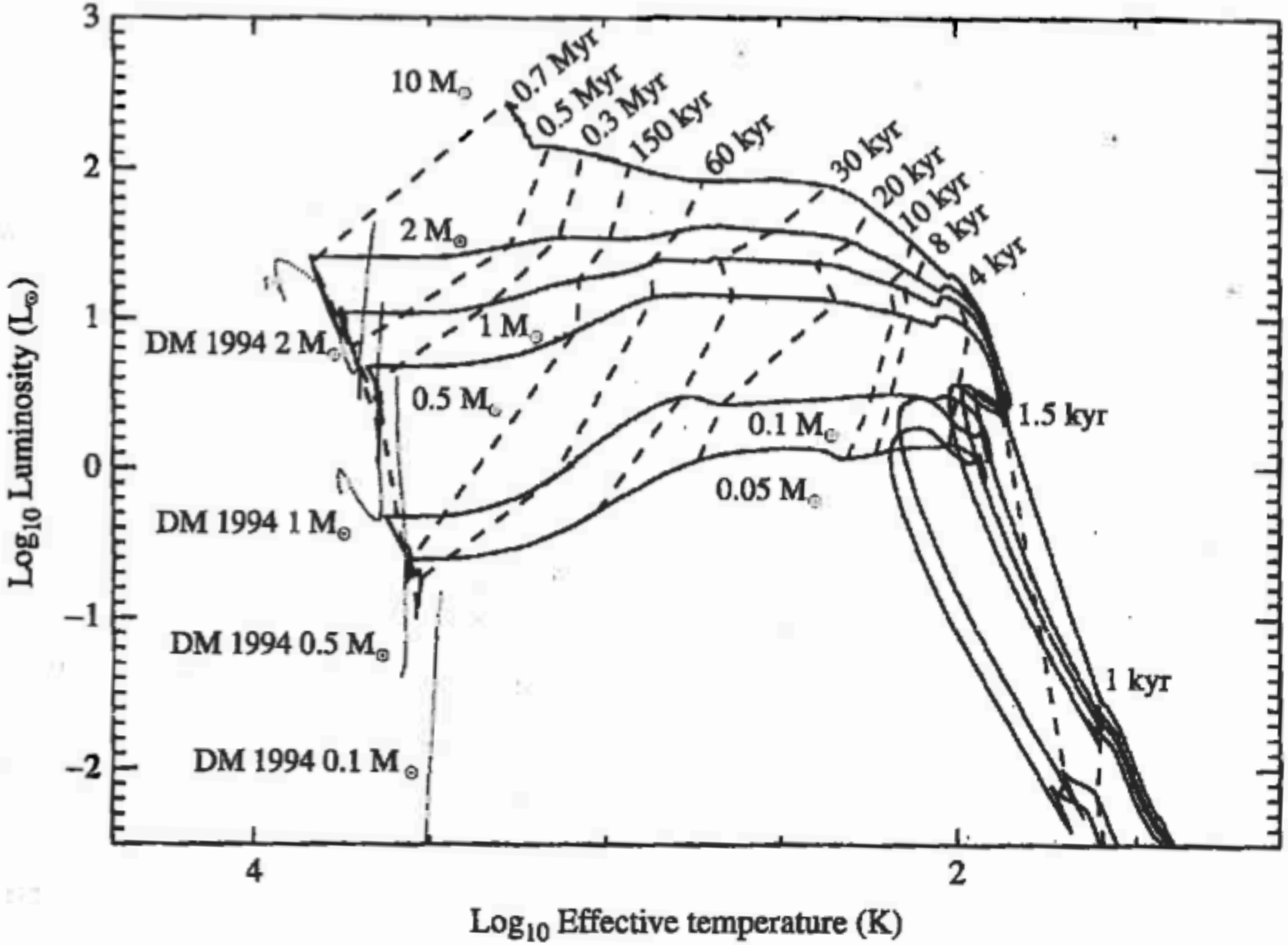

FIGURE 12.9 Theoretical evolutionary tracks of the gravitational collapse of 0.05, 0.1, 0.5, 1, 2, and 10 $M_\odot$ clouds through the protostar phase (solid lines). The dashed lines show the times since collapse began. The light dotted lines are pre-main-sequence evolutionary tracks of 0.1, 0.5, 1, and 2 $M_\odot$ stars from D'Antona and Mazzitelli, *Ap. J. Suppl.*, *90*, 457, 1994. Note that the horizontal axis is plotted with effective temperature increasing to the left, as is characteristic of all H–R diagrams. (Figure adapted from Wuchterl and Tscharnuter, *Astron. Astrophys.*, *398*, 1081, 2003.)

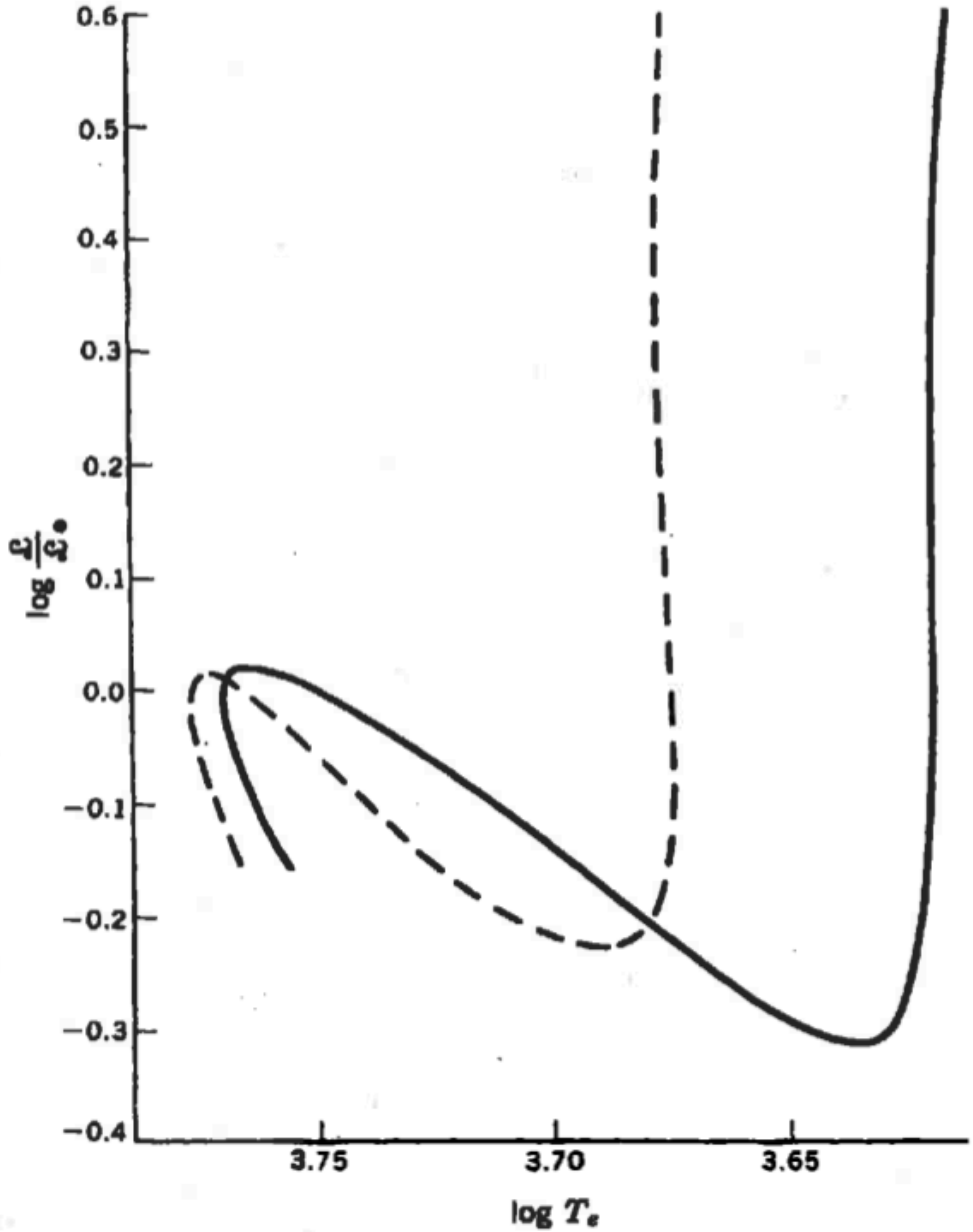

Fig. 6-6 Computed paths in the H-R diagram for the contraction of a one-solar-mass star to the main sequence. The two tracks shown differ only in the metal abundance, which affects the structure of such stars by virtue of its effect on the surface opacity. The solid curve corresponds to a metallic mass fraction $X_M = 5.4 \times 10^{-3}$, and the dashed curve corresponds to $X_M = 5.4 \times 10^{-6}$. [*After I. Iben, Jr., Astrophys. J.*, **141**: 993 (1965). *By permission of The University of Chicago Press. Copyright* 1965 *by The University of Chicago.*]

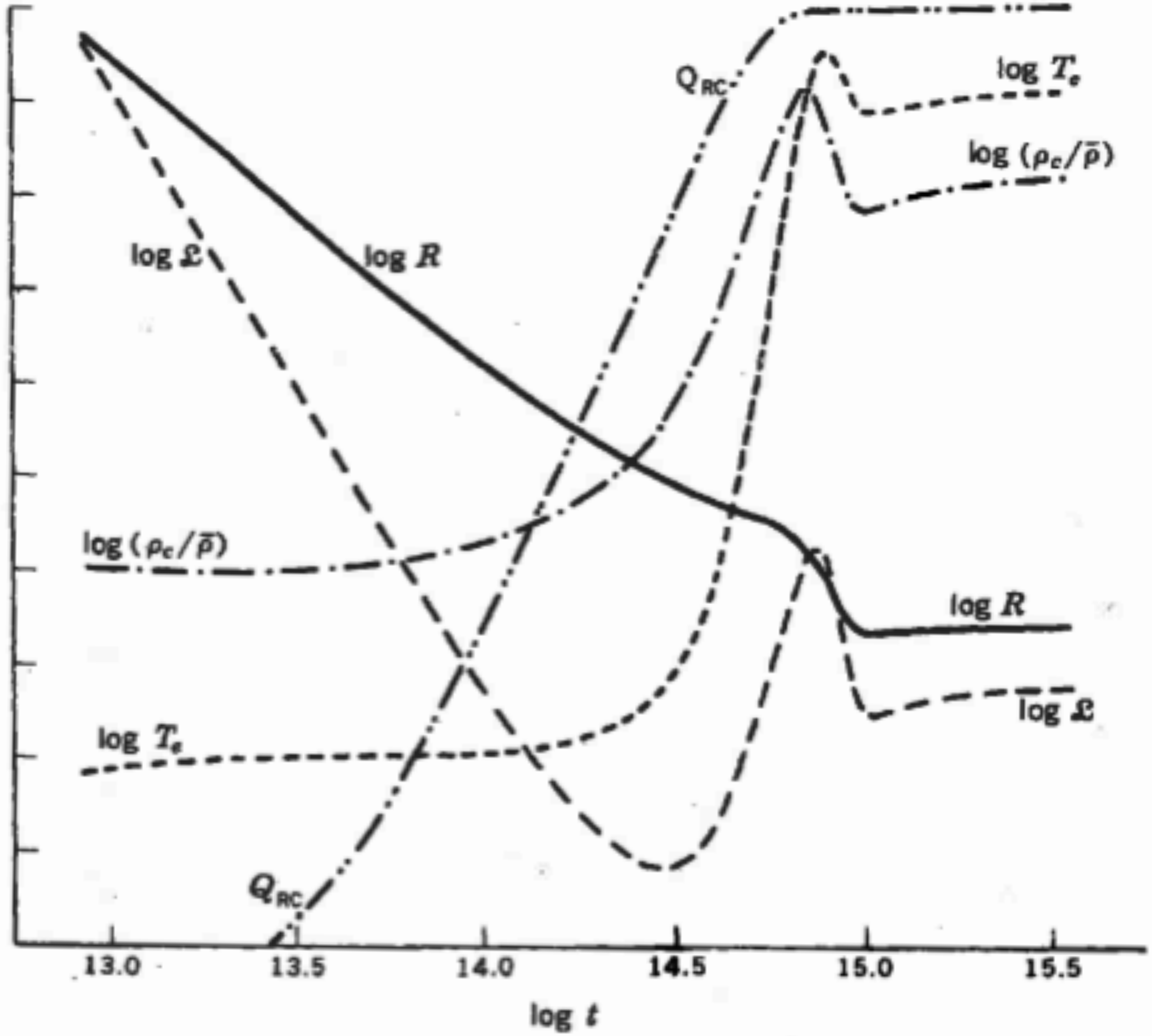

Fig. 6-7 The variation with time t (in seconds) of the surface temperature, the luminosity, the radius, the ratio of central density to mean density, and the mass fraction Q_{RC} within the radiative core during the contraction of a one-solar-mass star to the main sequence. The full-scale limits correspond to $3.78 > \log T_e > 3.58$, $0.6 > \log (\mathcal{L}/\mathcal{L}_\odot) > -0.4$, $0.6 > \log (R/R_\odot) > -0.4$, $2.0 > \log (\rho_c/\bar{\rho}) > 0$, and $1 > Q_{RC} > 0$. [*After I. Iben, Jr., Astrophys. J.*, **141**:993 (1965). *By permission of The University of Chicago Press. Copyright* 1965 *by The University of Chicago.*]

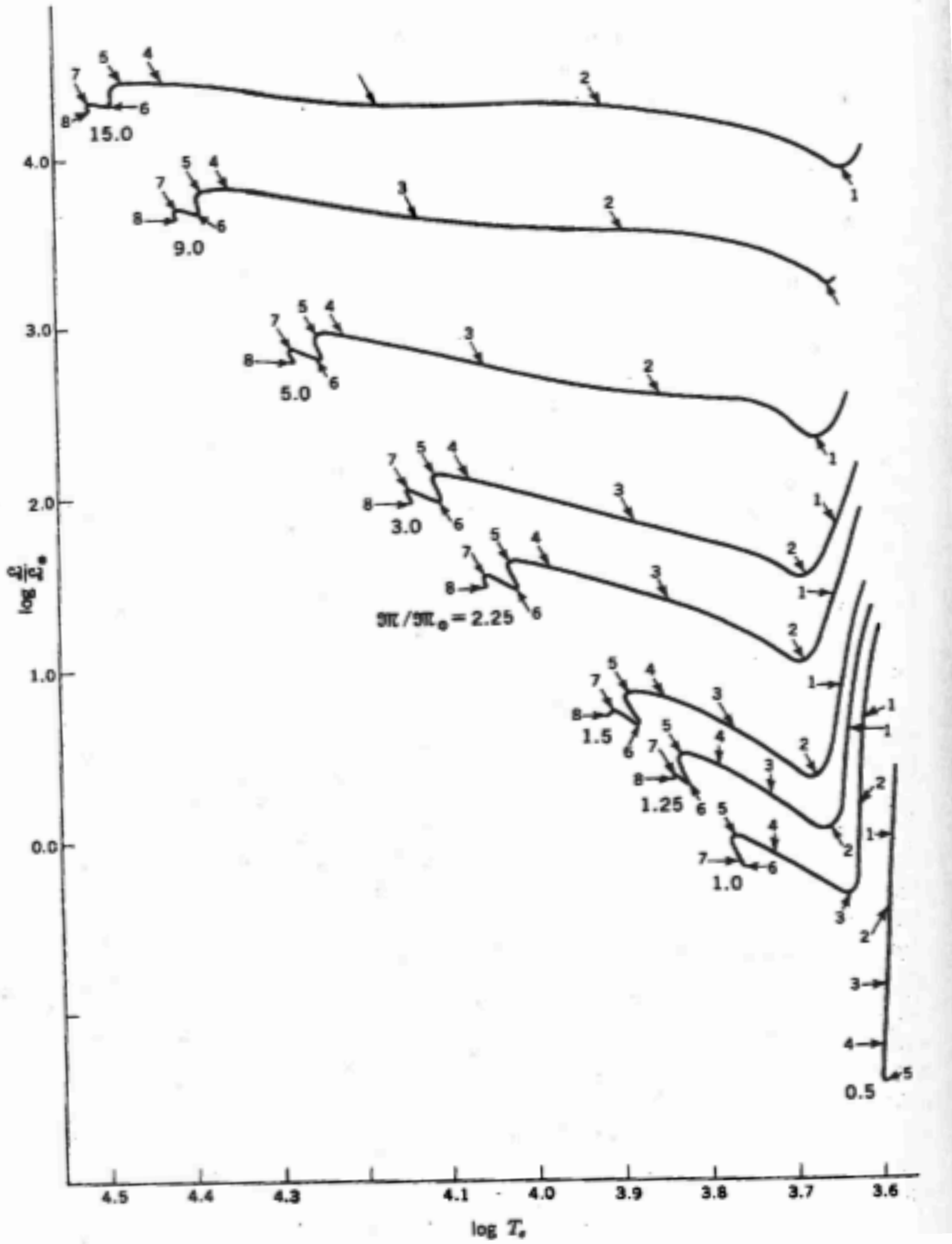

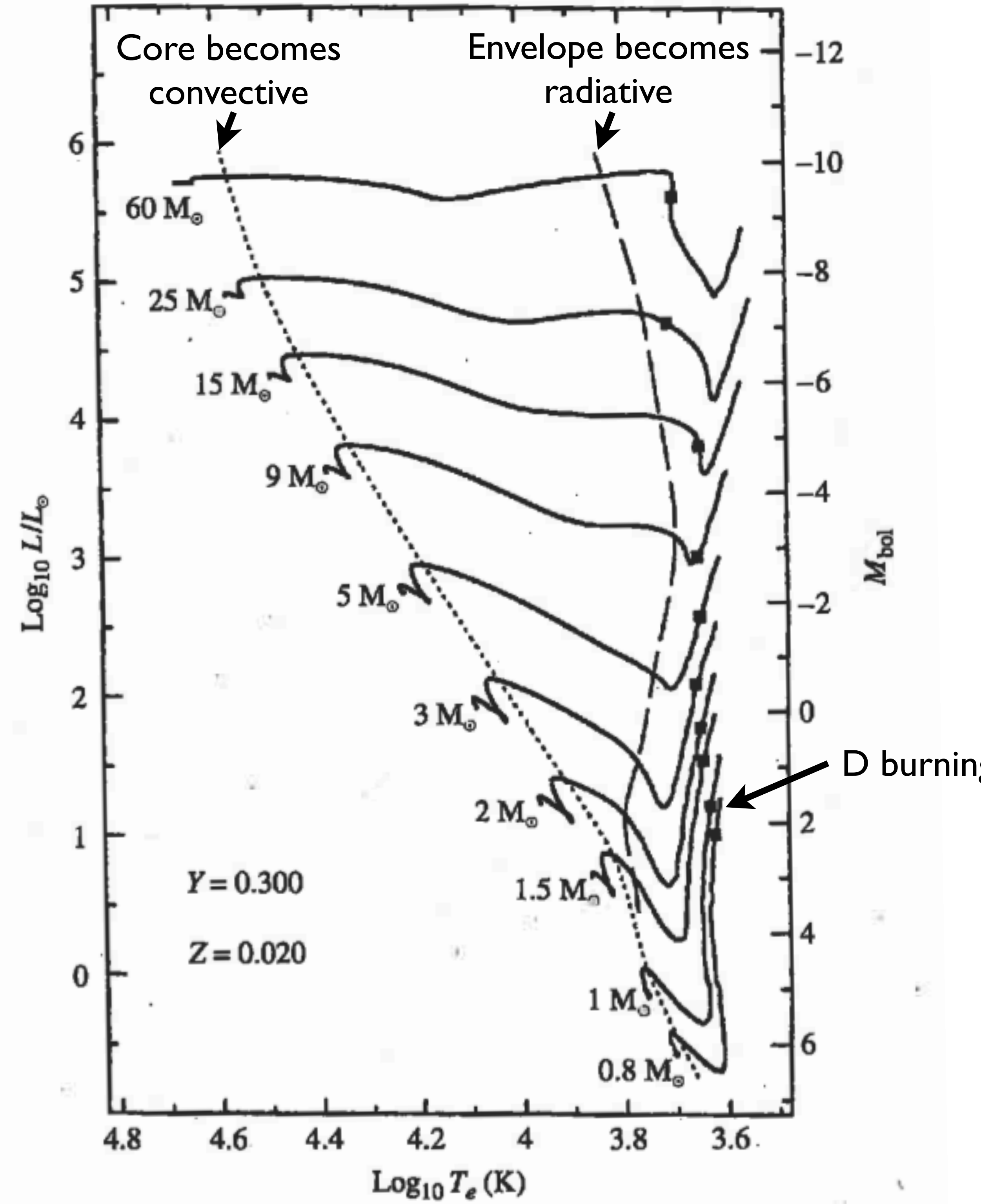

Table 6-1 Evolutionary lifetimes, years†

	$\mathfrak{M}/\mathfrak{M}_\odot$								
Point	15.0	9.0	5.0	3.0	2.25	1.5	1.25	1.0	0.5
1	6.740×10^3	1.443×10^3	2.936×10^4	3.420×10^4	7.862×10^4	2.347×10^5	4.508×10^5	1.189×10^5	3.195×10^5
2	3.766×10^3	1.473×10^4	1.069×10^5	2.078×10^5	5.940×10^5	2.363×10^6	3.957×10^6	1.058×10^6	1.786×10^6
3	9.350×10^3	3.645×10^4	2.001×10^5	7.633×10^5	1.883×10^6	5.801×10^6	8.800×10^6	8.910×10^6	8.711×10^6
4	2.203×10^4	6.987×10^4	2.860×10^5	1.135×10^6	2.505×10^6	7.584×10^6	1.155×10^7	1.821×10^7	3.092×10^7
5	2.657×10^4	7.922×10^4	3.137×10^5	1.250×10^6	2.818×10^6	8.620×10^6	1.404×10^7	2.529×10^7	1.550×10^8
6	3.984×10^4	1.019×10^5	3.880×10^5	1.465×10^6	3.319×10^6	1.043×10^7	1.755×10^7	3.418×10^7	
7	4.585×10^4	1.195×10^5	4.559×10^5	1.741×10^6	3.993×10^6	1.339×10^7	2.796×10^7	5.016×10^7	
8	6.170×10^4	1.505×10^5	5.759×10^5	2.514×10^6	5.855×10^6	1.821×10^7	2.954×10^7		

† I. Iben, Jr., *Astrophys. J.*, **141**:993 (1965). By permission of The University of Chicago Press.

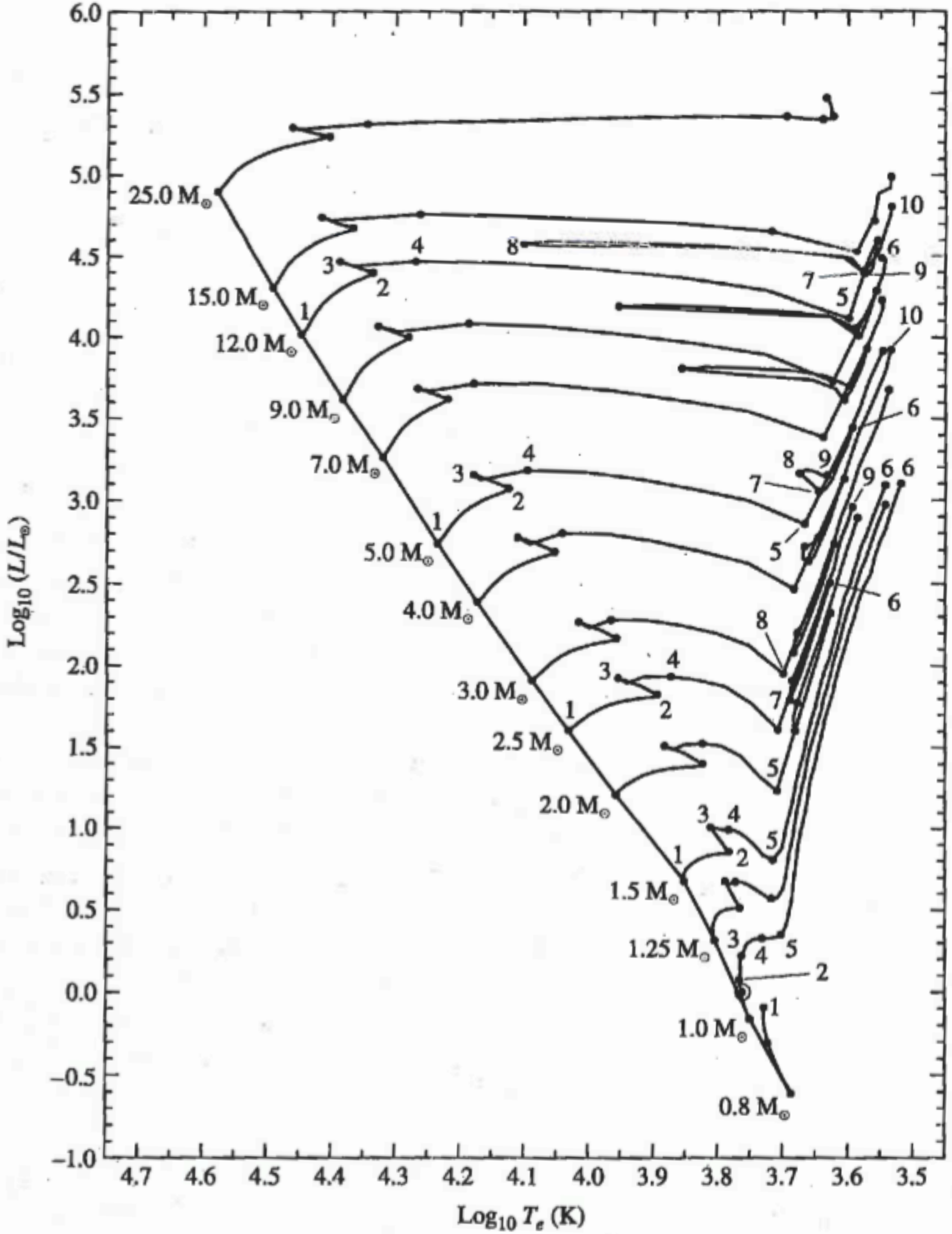

6.0
5.5
5.0
4.5
4.0
3.5
3.0
2.5
2.0
1.5
1.0
0.5
0.0
−0.5
−1.0
4.7
4.6
4.5
4.4
4.3
4.2
4.1
4.0
3.9
3.8
3.7
3.6
3.5
Log10 (L/L⊙)
Log10 Te (K)
25.0 M⊙
15.0 M⊙
12.0 M⊙
9.0 M⊙
7.0 M⊙
5.0 M⊙
4.0 M⊙
3.0 M⊙
2.5 M⊙
2.0 M⊙
1.5 M⊙
1.25 M⊙
1.0 M⊙
0.8 M⊙
1
2
3
4
5
6
7
8
9
10

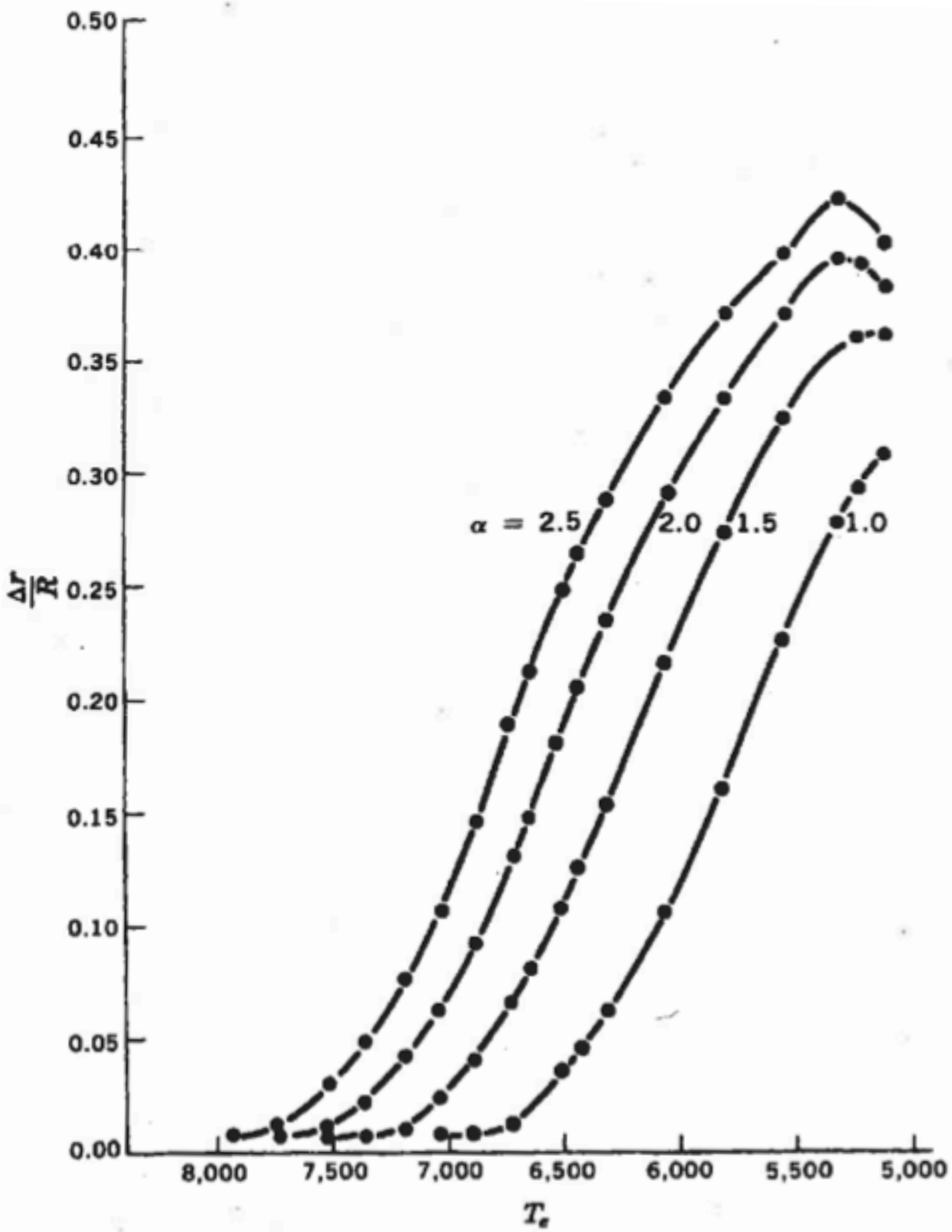

Fig. 6-9 Depth of the outer convection zone of main-sequence stars as a function of T_e. The four separate curves were computed for four different choices of the mixing-length parameter α. [*After N. Baker, The Depth of the Outer Convection Zone in Main-sequence Stars, Inst. Space Studies Rept., New York* (undated).]

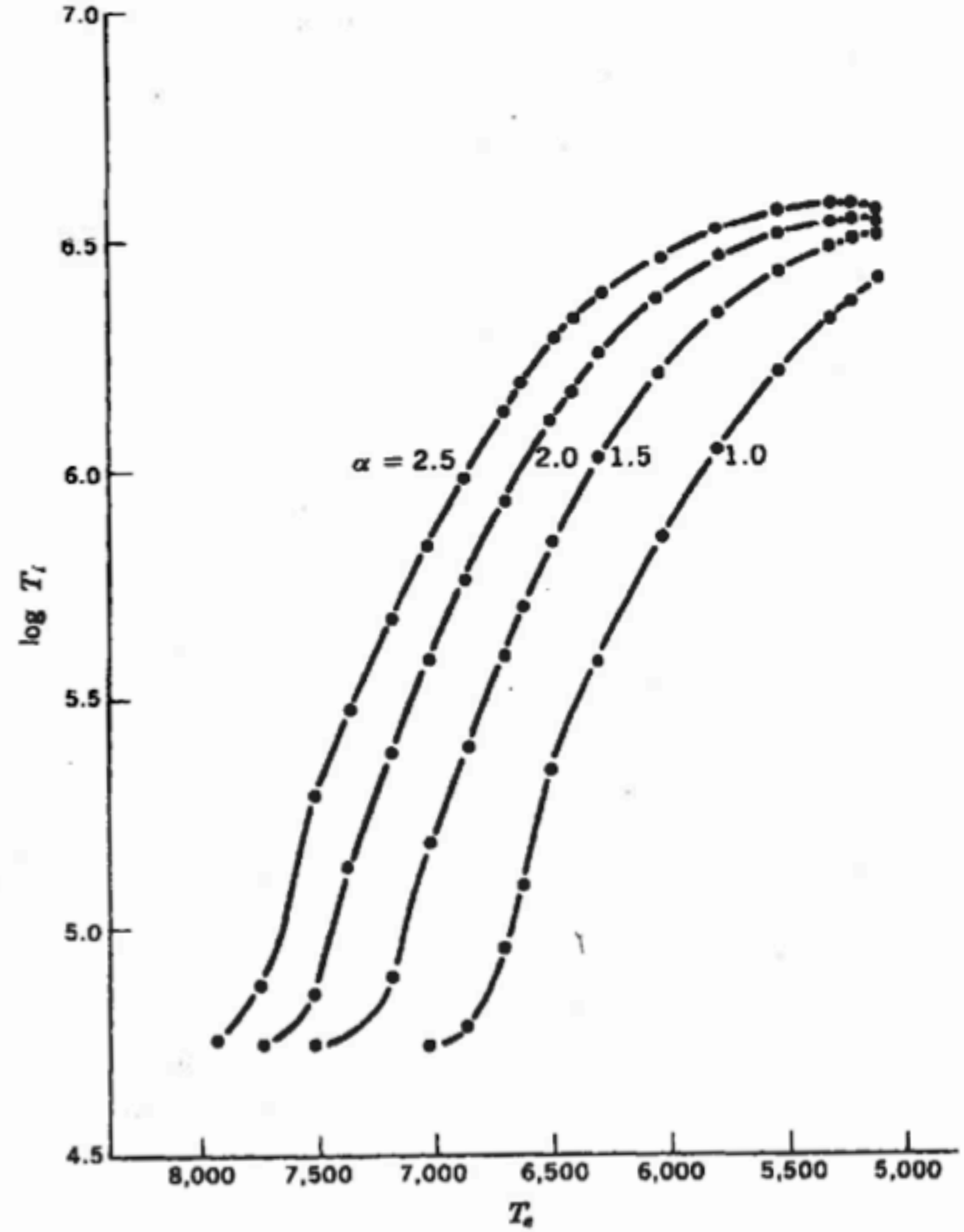

Fig. 6-10 The temperature T_i at the base of the outer convection zone as a function of T_e. [*After N. Baker, The Depth of the Outer Convection Zone in Main-sequence Stars, Inst. Space Studies Rept., New York* (undated).]

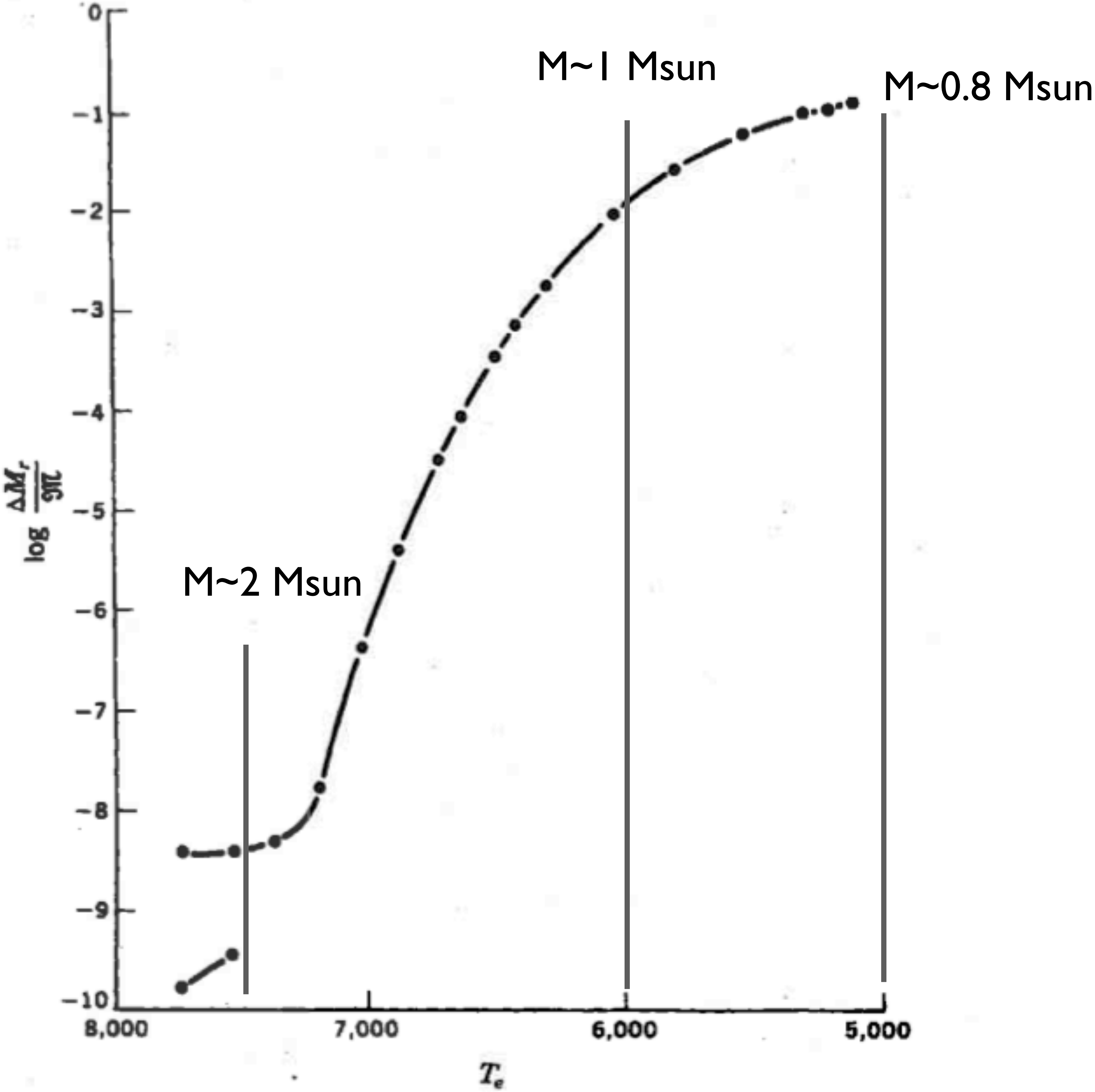

Fig. 6-11 The fraction of the stellar mass contained in the outer convection zone of a main-sequence star as a function of T_e. [*After N. Baker, The Depth of the Outer Convection Zone in Main-sequence Stars, Inst. Space Studies Rept., New York* (*undated*).]

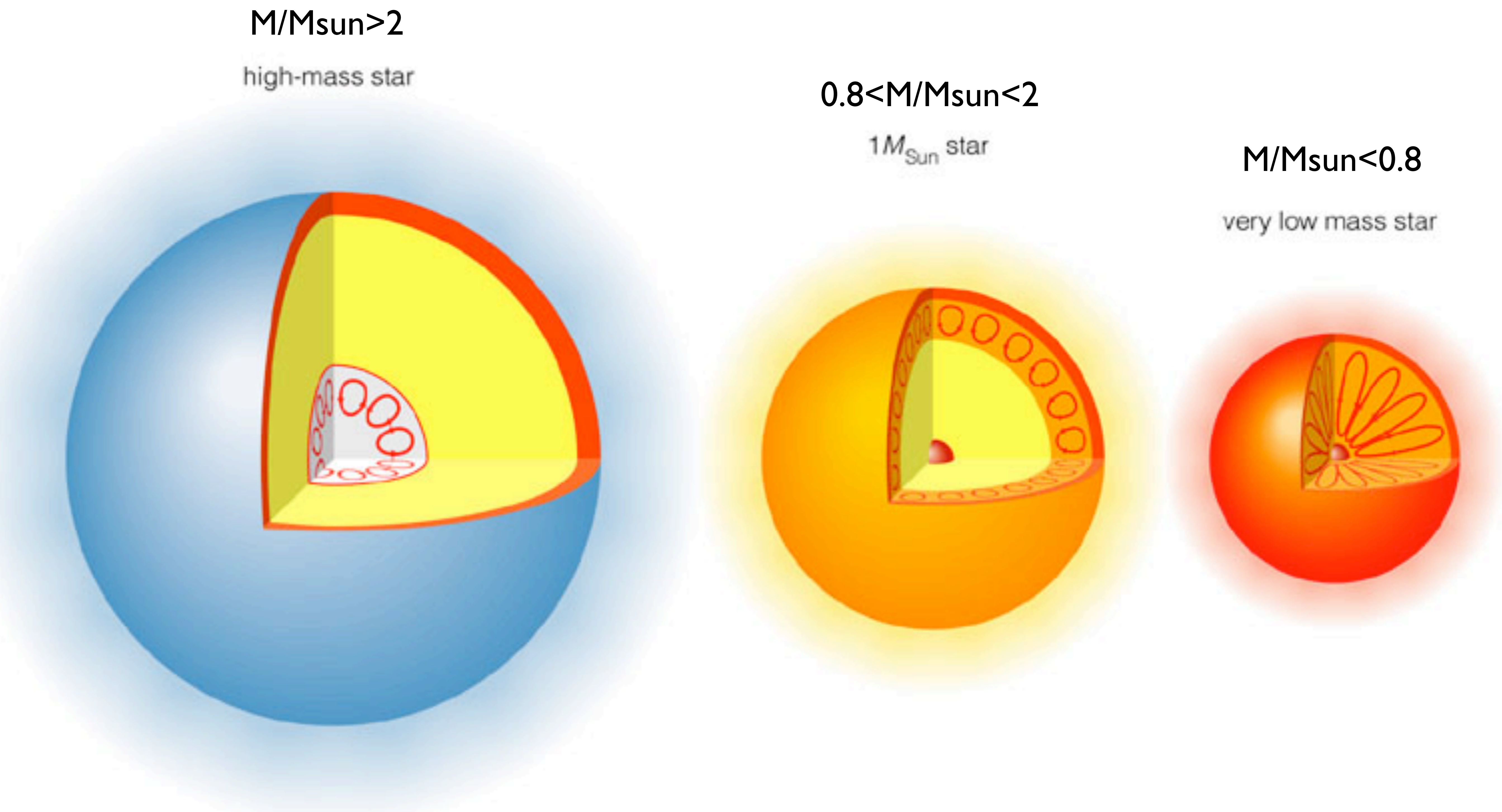
M/Msun>2
high-mass star
0.8<M/Msun<2
1M_{Sun} star
M/Msun<0.8
very low mass star

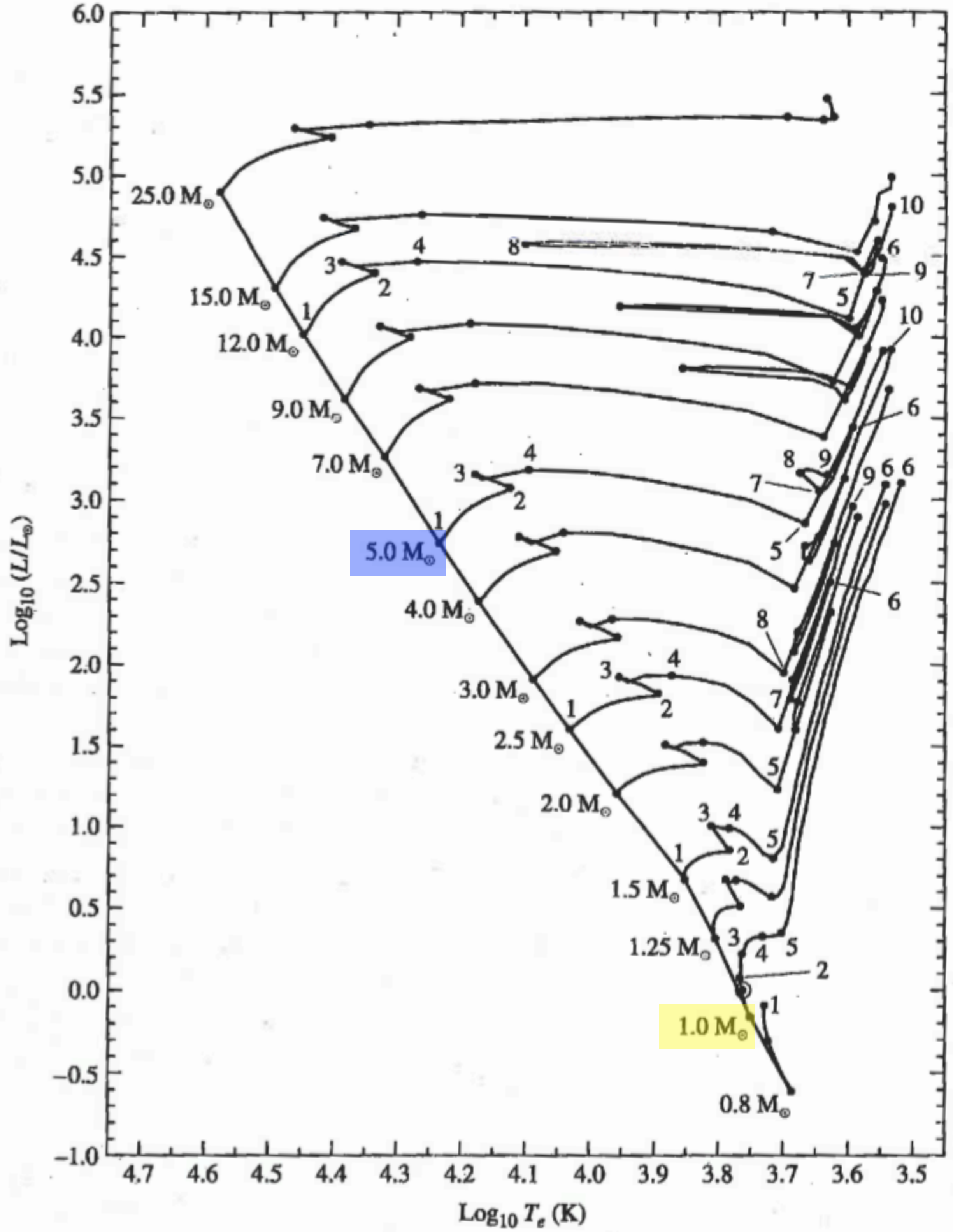

FIGURE 13.1 Main-sequence and post-main-sequence evolutionary tracks of stars with an initial composition of $X = 0.68$, $Y = 0.30$, and $Z = 0.02$. The location of the present-day Sun (see Fig. 13.2) is depicted by the solar symbol (⊙) between points 1 and 2 on the 1 $M_\odot$ track. The elapsed times to points indicated on the diagram are given in Table 13.1. To enhance readability, only the points on the evolutionary tracks for 0.8, 1.0, 1.5, 2.5, 5.0, and 12.0 $M_\odot$ are labeled. The model calculations include mass loss and convective overshooting. The diagonal line connecting the locus of points 1 is the zero-age main sequence. For complete, and annotated, evolutionary tracks of 1 $M_\odot$ and 5 $M_\odot$ stars, see Figs. 13.4 and 13.5, respectively. (Data from Schaller et al., *Astron. Astrophys. Suppl.*, *96*, 269, 1992.)

TABLE 13.1 The elapsed times since reaching the zero-age main sequence to the indicated points in Fig. 13.1, measured in millions of years (Myr). (Data from Schaller et al., *Astron. Astrophys. Suppl.*, *96*, 269, 1992.)

Initial Mass ($M_\odot$)	1 6	2 7	3 8	4 9	5 10
25	0	6.33044	6.40774	6.41337	6.43767
	6.51783	7.04971	7.0591		
15	0	11.4099	11.5842	11.5986	11.6118
	11.6135	11.6991	12.7554		
12	0	15.7149	16.0176	16.0337	16.0555
	16.1150	16.4230	16.7120	17.5847	17.6749
9	0	25.9376	26.3886	26.4198	26.4580
	26.5019	27.6446	28.1330	28.9618	29.2294
7	0	42.4607	43.1880	43.2291	43.3388
	43.4304	45.3175	46.1810	47.9727	48.3916
5	0	92.9357	94.4591	94.5735	94.9218
	95.2108	99.3835	100.888	107.208	108.454
4	0	162.043	164.734	164.916	165.701
	166.362	172.38	185.435	192.198	194.284
3	0	346.240	352.503	352.792	355.018
	357.310	366.880	420.502	440.536	
2.5	0	574.337	584.916	586.165	589.786
	595.476	607.356	710.235	757.056	
2	0	1094.08	1115.94	1117.74	1129.12
	1148.10	1160.96	1379.94	1411.25	
1.5	0	2632.52	2690.39	2699.52	2756.73
	2910.76				
1.25	0	4703.20	4910.11	4933.83	5114.83
	5588.92				
1	0	7048.40	9844.57	11386.0	11635.8
	12269.8				
0.8	0	18828.9	25027.9		

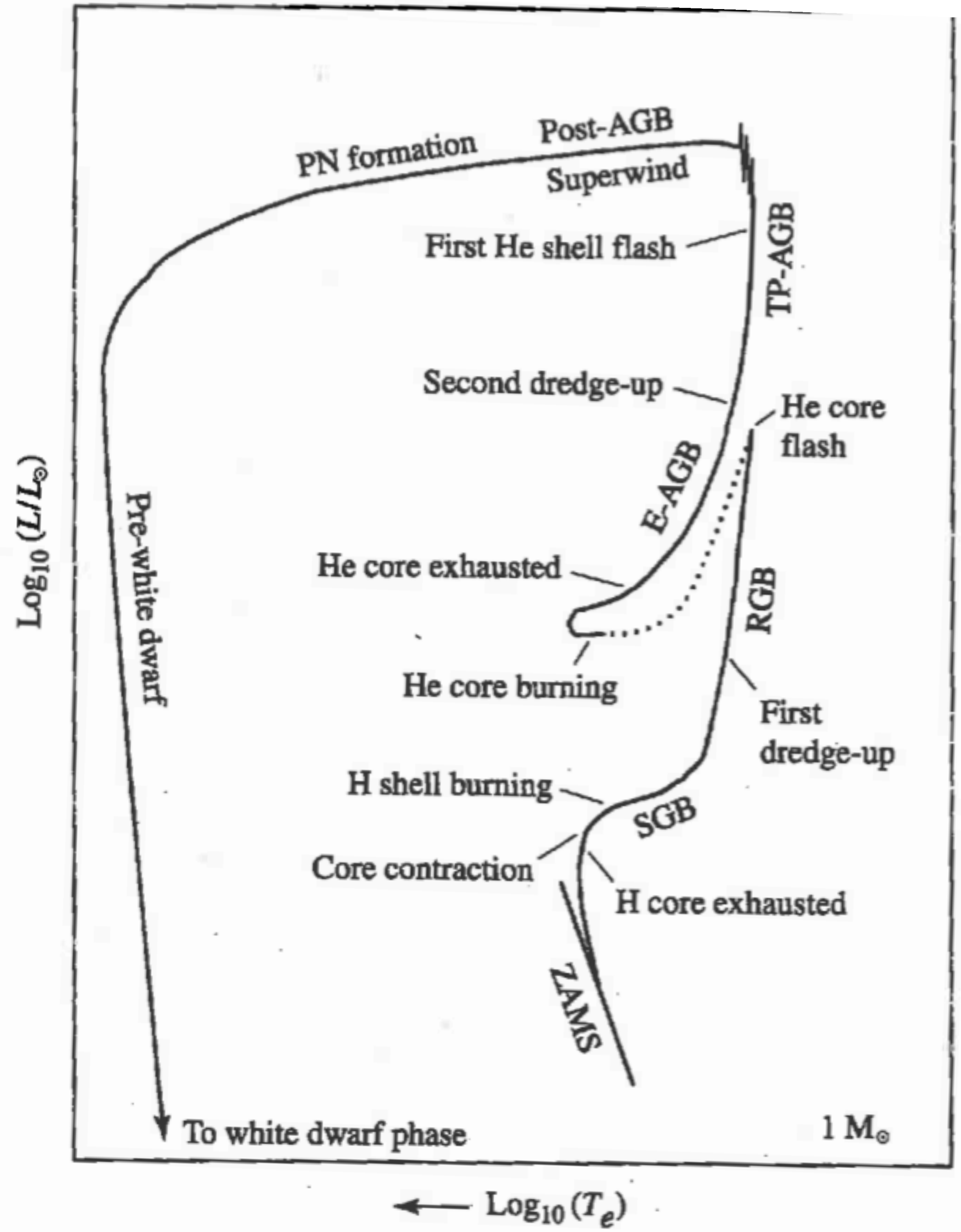

FIGURE 13.4 A schematic diagram of the evolution of a low-mass star of 1 $M_\odot$ from the zero-age main sequence to the formation of a white dwarf star (see Section 16.1). The dotted phase of evolution represents rapid evolution following the helium core flash. The various phases of evolution are labeled as follows: Zero-Age-Main-Sequence (ZAMS), Sub-Giant Branch (SGB), Red Giant Branch (RGB), Early Asymptotic Giant Branch (E-AGB), Thermal Pulse Asymptotic Giant Branch (TP-AGB), Post-Asymptotic Giant Branch (Post-AGB), Planetary Nebula formation (PN formation), and Pre-white dwarf phase leading to white dwarf phase.

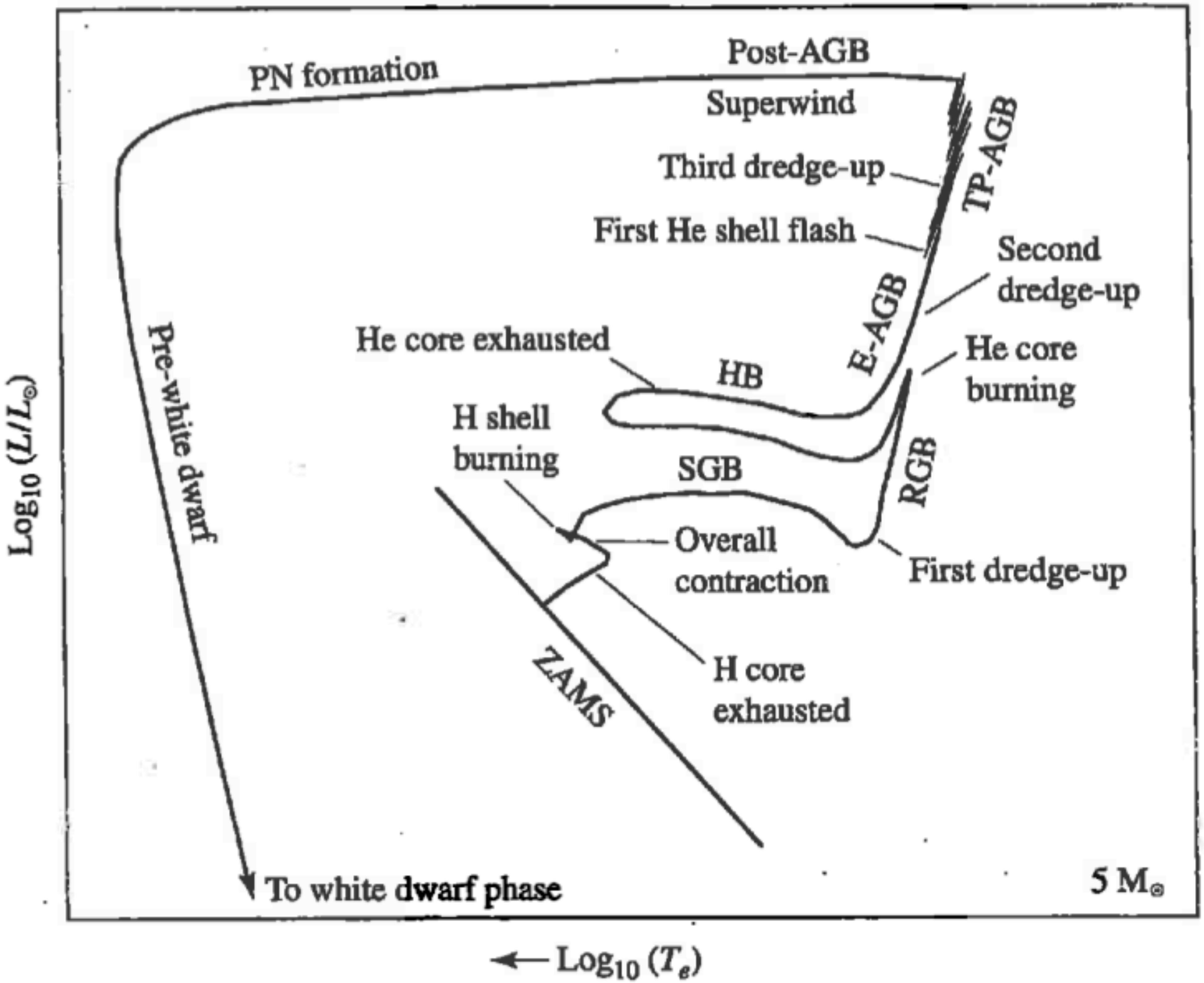

FIGURE 13.5 A schematic diagram of the evolution of an intermediate-mass star of 5 $M_\odot$ from the zero-age main sequence to the formation of a white dwarf star (see Section 16.1). The diagram is labeled according to Fig. 13.4 with the addition of the Horizontal Branch (HB).

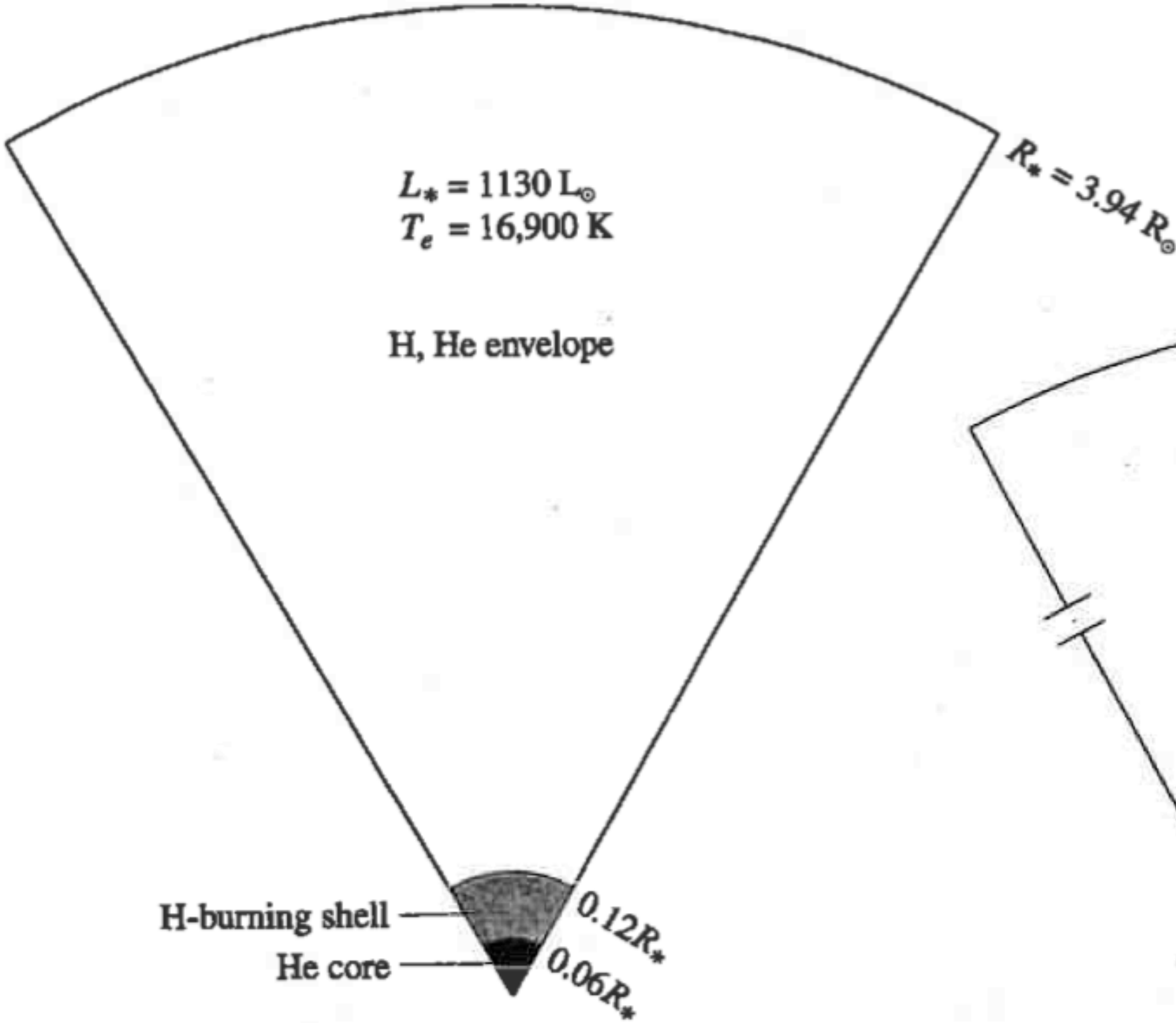

5 Msun star with He core and H-burning shell shortly after shell ignition

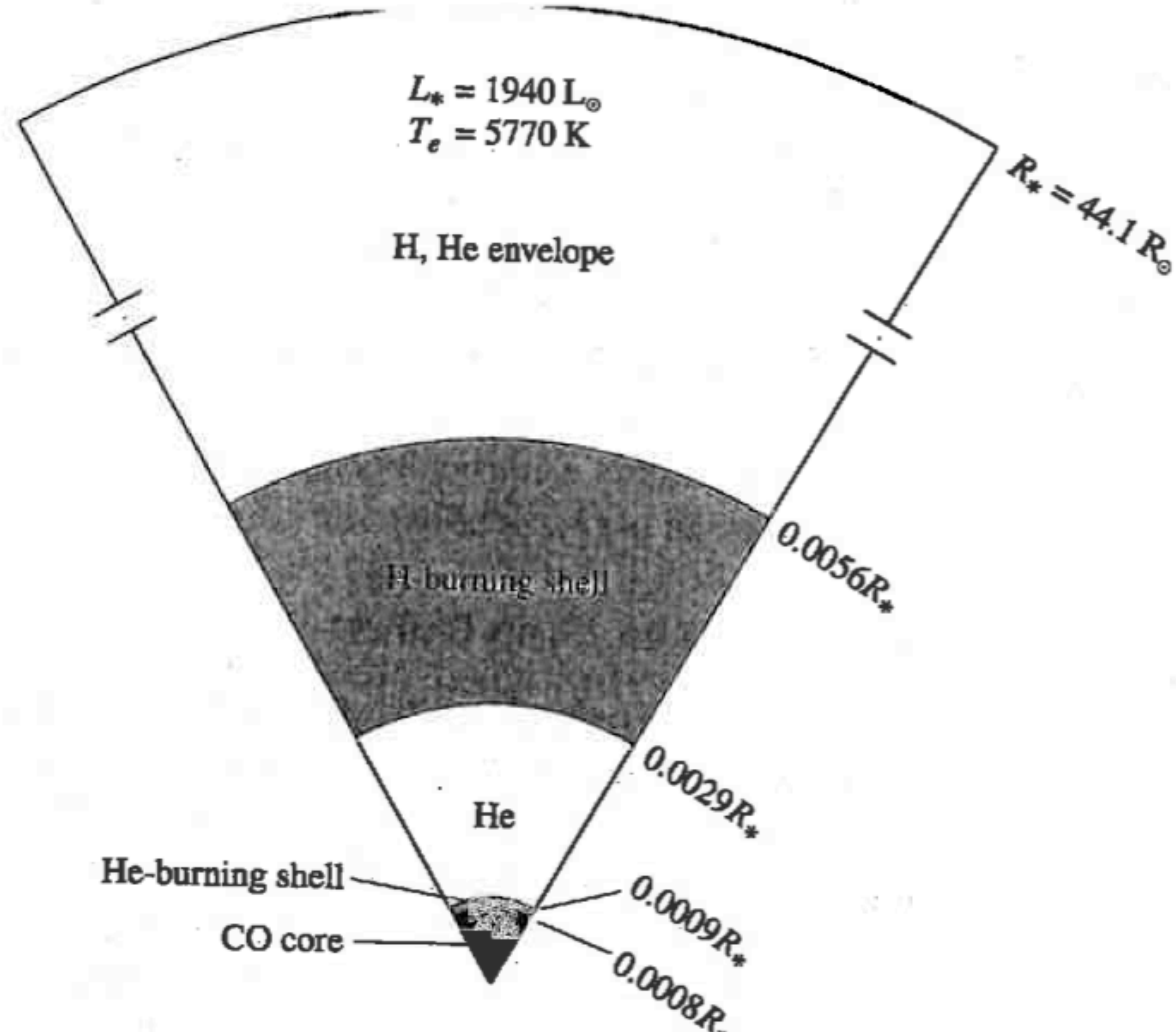

5 Msun star on the early asymptotic giant branch with C-O core and H- and He-burning shells. The scale of the shells and core has been increased by x100.

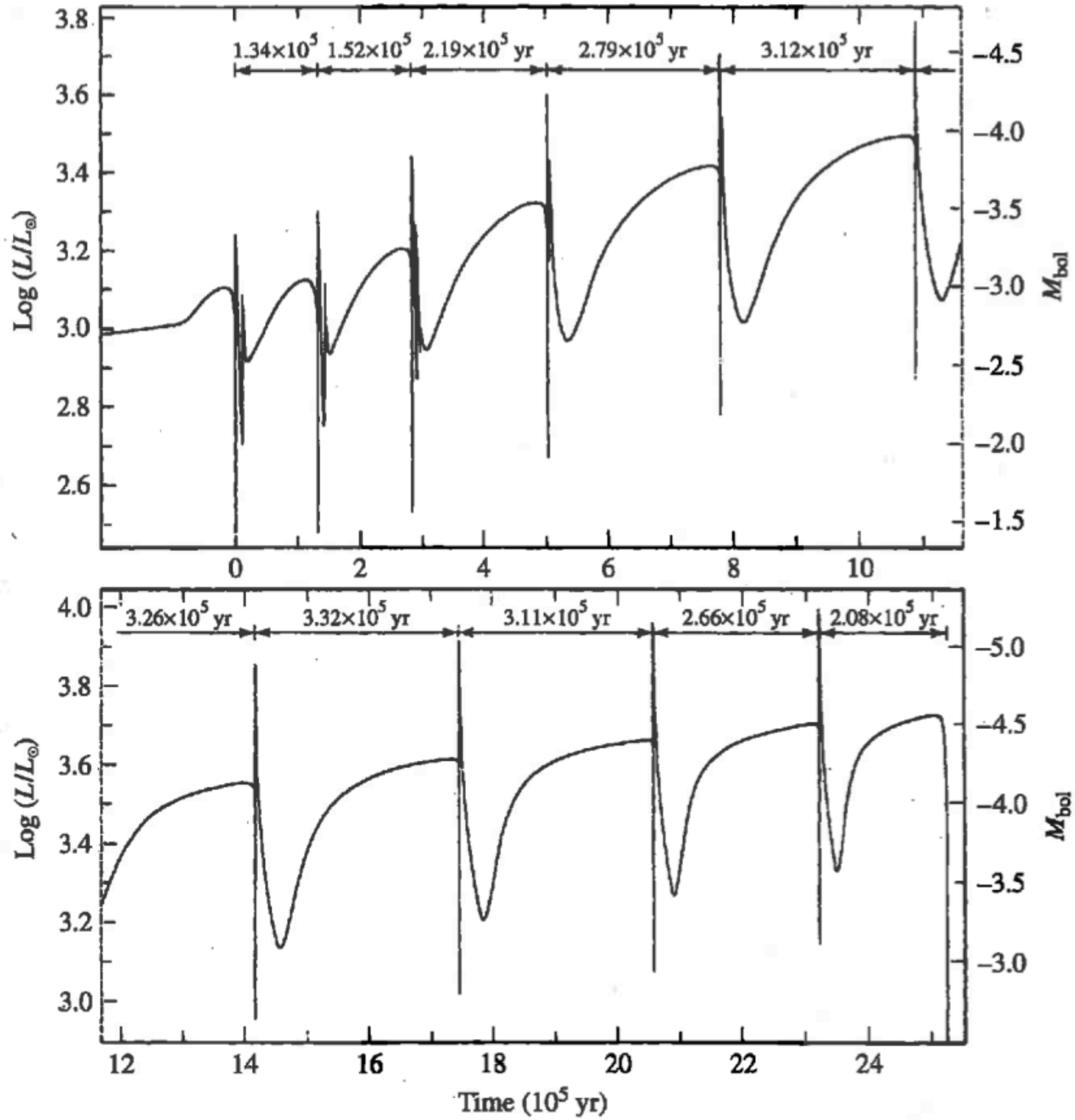

FIGURE 13.9 The surface luminosity as a function of time for a 0.6 $M_\odot$ stellar model that is undergoing helium shell flashes on the TP-AGB. (Figure adapted from Iben, *Ap. J.*, *260*, 821, 1982.)

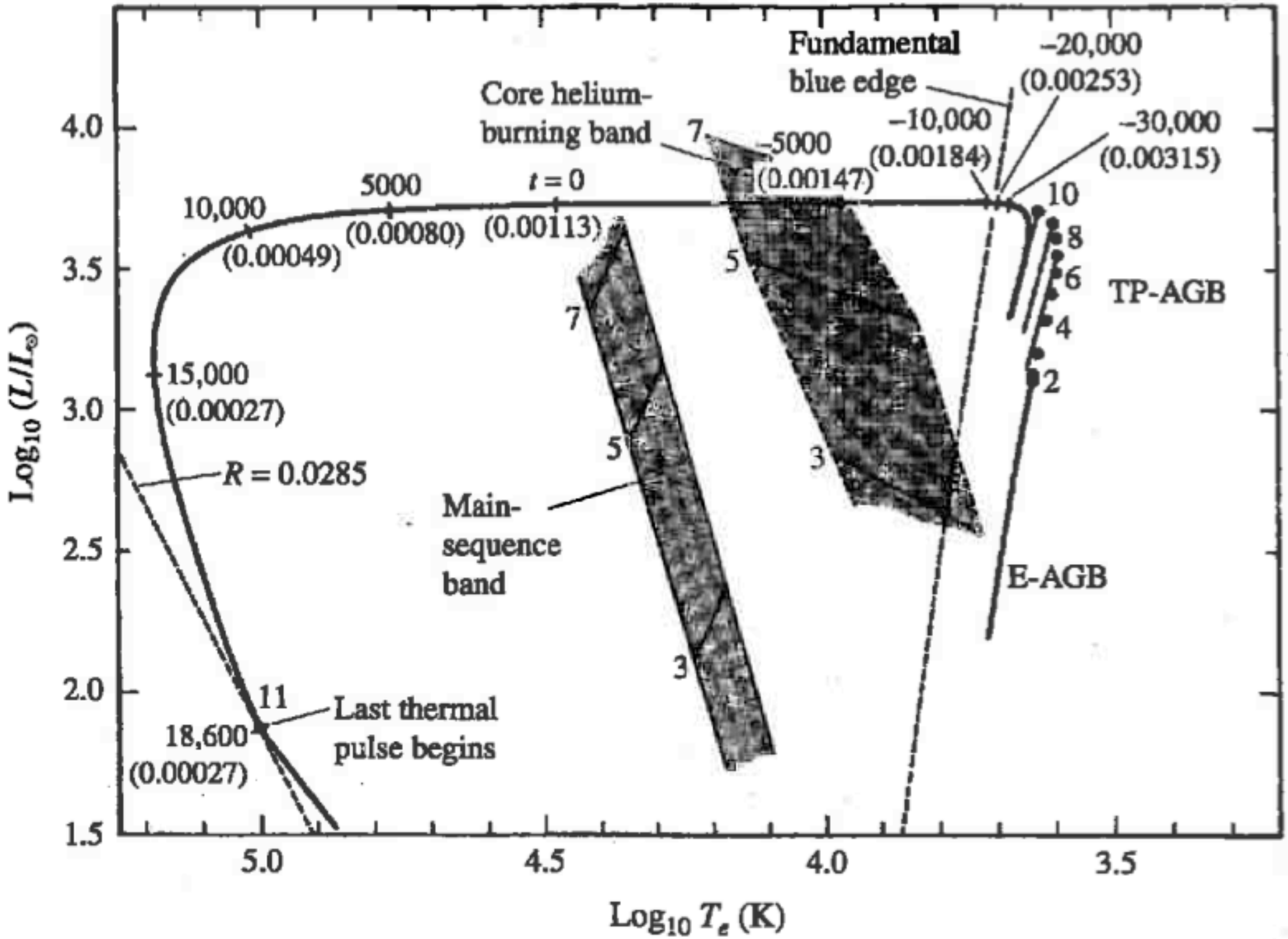

FIGURE 13.12 The AGB and post-AGB evolution of a 0.6 $M_\odot$ star undergoing mass loss. The initial composition of the model is $X = 0.749$, $Y = 0.25$, and $Z = 0.001$. The main-sequence and horizontal branches of 3, 5, and 7 $M_\odot$ stars are shown for reference. Details of the figure are discussed in the body of the text. (Figure adapted from Iben, *Ap. J.*, *260*, 821, 1982.)


Planetary Nebula IC 418
Hubble Heritage
PRC00-28 • NASA and The Hubble Heritage Team (STScI/AURA) • HST/WFPC2


Henize 1357 • Stingray Nebula
Hubble Space Telescope • WFPC2
PRC98-15 • ST ScI OPO • April 2, 1998 • M. Bobrowsky (Orbital Sciences Corp.) and NASA


Planetary Nebulae • Hubble Space Telescope • WFPC2
He 2-47
NGC 5315
IC 4593
NGC 5307
NASA, ESA, and The Hubble Heritage Team (STScI/AURA) • STScI-PRC07-33a

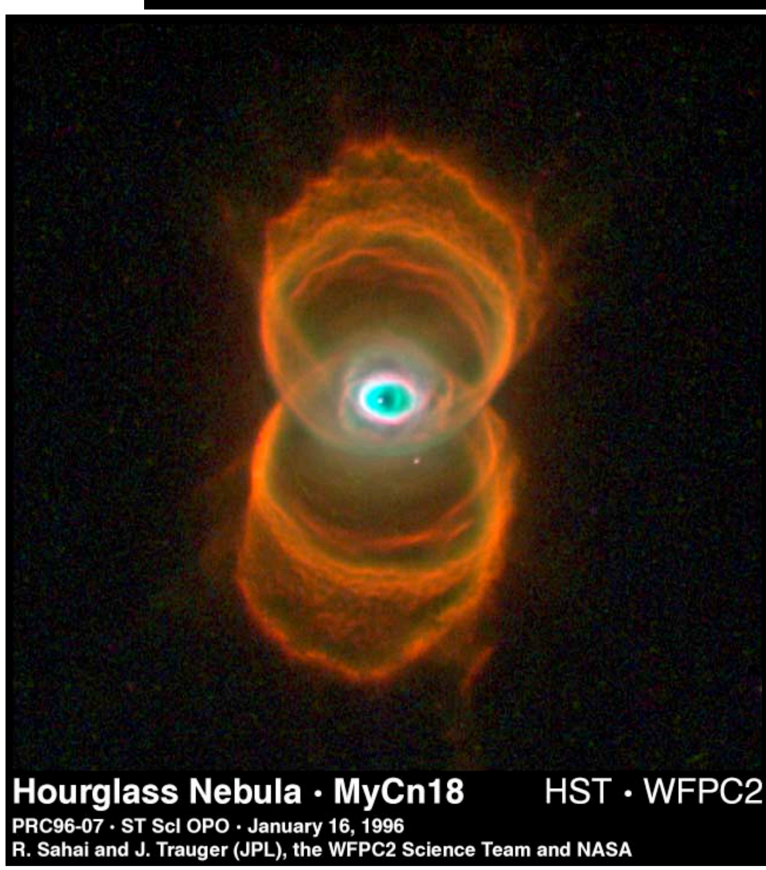
Hourglass Nebula • MyCn18
HST • WFPC2
PRC96-07 • ST ScI OPO • January 16, 1996
R. Sahai and J. Trauger (JPL), the WFPC2 Science Team and NASA

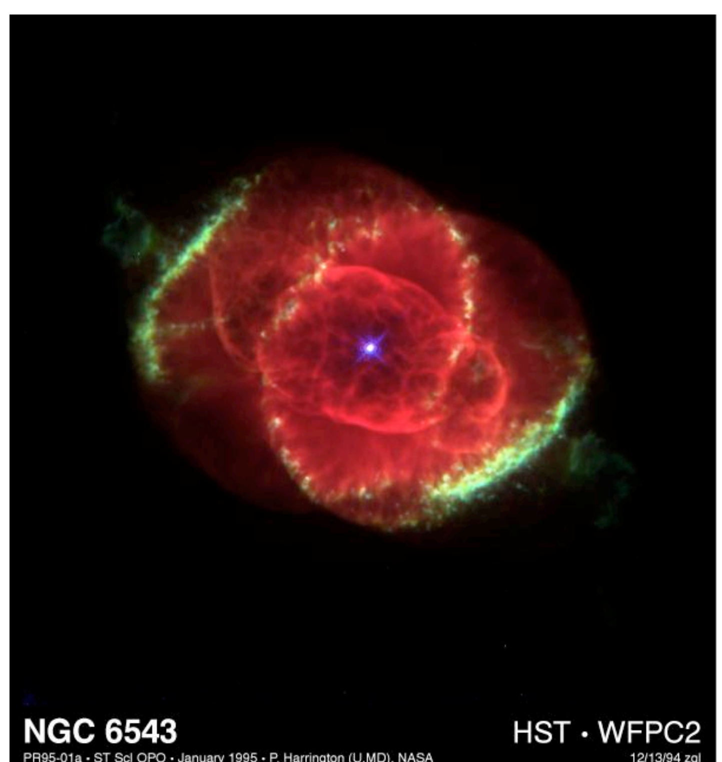
NGC 6543
HST • WFPC2
PR95-01a • ST ScI OPO • January 1995 • P. Harrington (U.MD), NASA
12/13/94 zgl

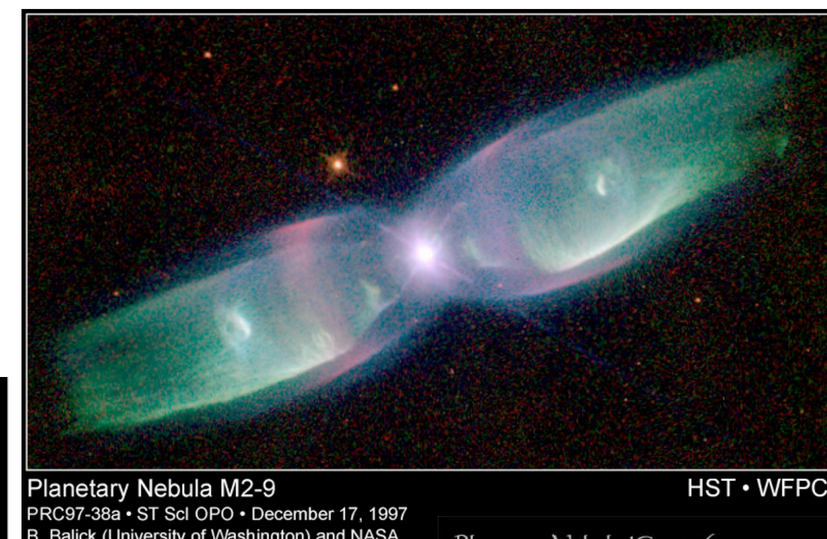
Planetary Nebula M2-9
HST • WFPC2
PRC97-38a • ST ScI OPO • December 17, 1997
B. Balick (University of Washington) and NASA

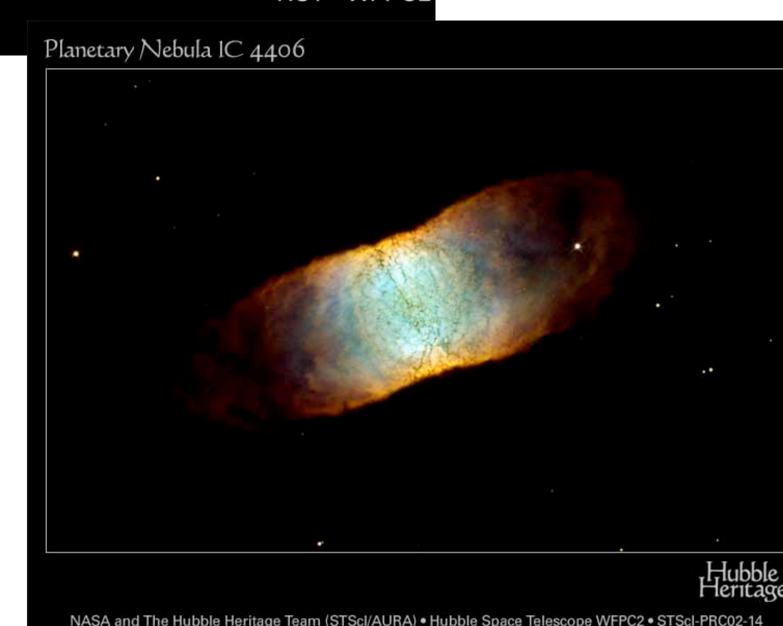
Planetary Nebula IC 4406
Hubble Heritage
NASA and The Hubble Heritage Team (STScI/AURA) • Hubble Space Telescope WFPC2 • STScI-PRC02-14

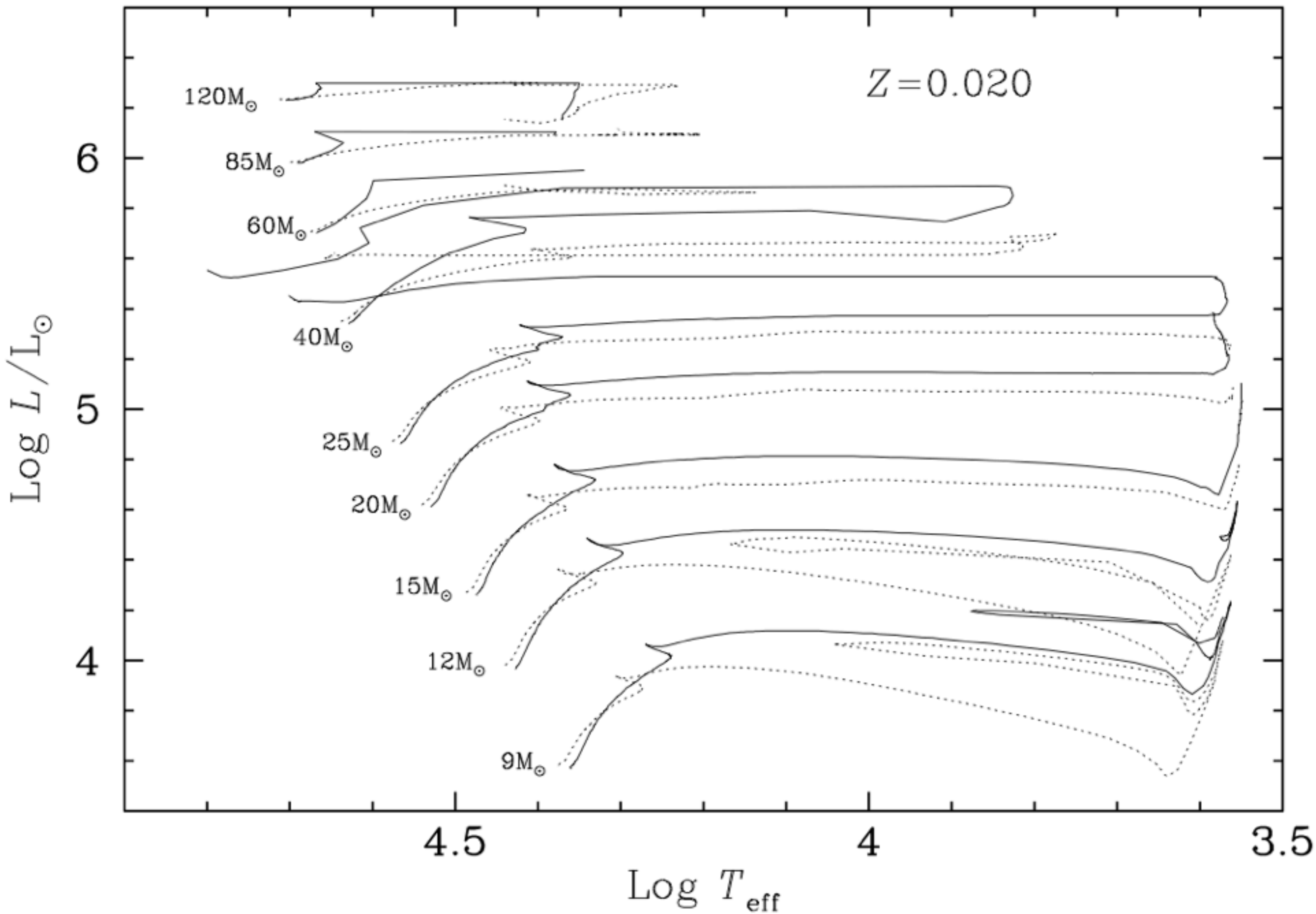

Fig. 5. Evolutionary tracks for non-rotating (dotted lines) and rotating (continuous lines) models for a metallicity Z = 0.020. The rotating models have an initial velocity $v_{\rm ini}$ of 300 km s^{-1}, which corresponds to an average velocity during the MS phase of about 180 to 240 km s^{-1} (see Table 1).

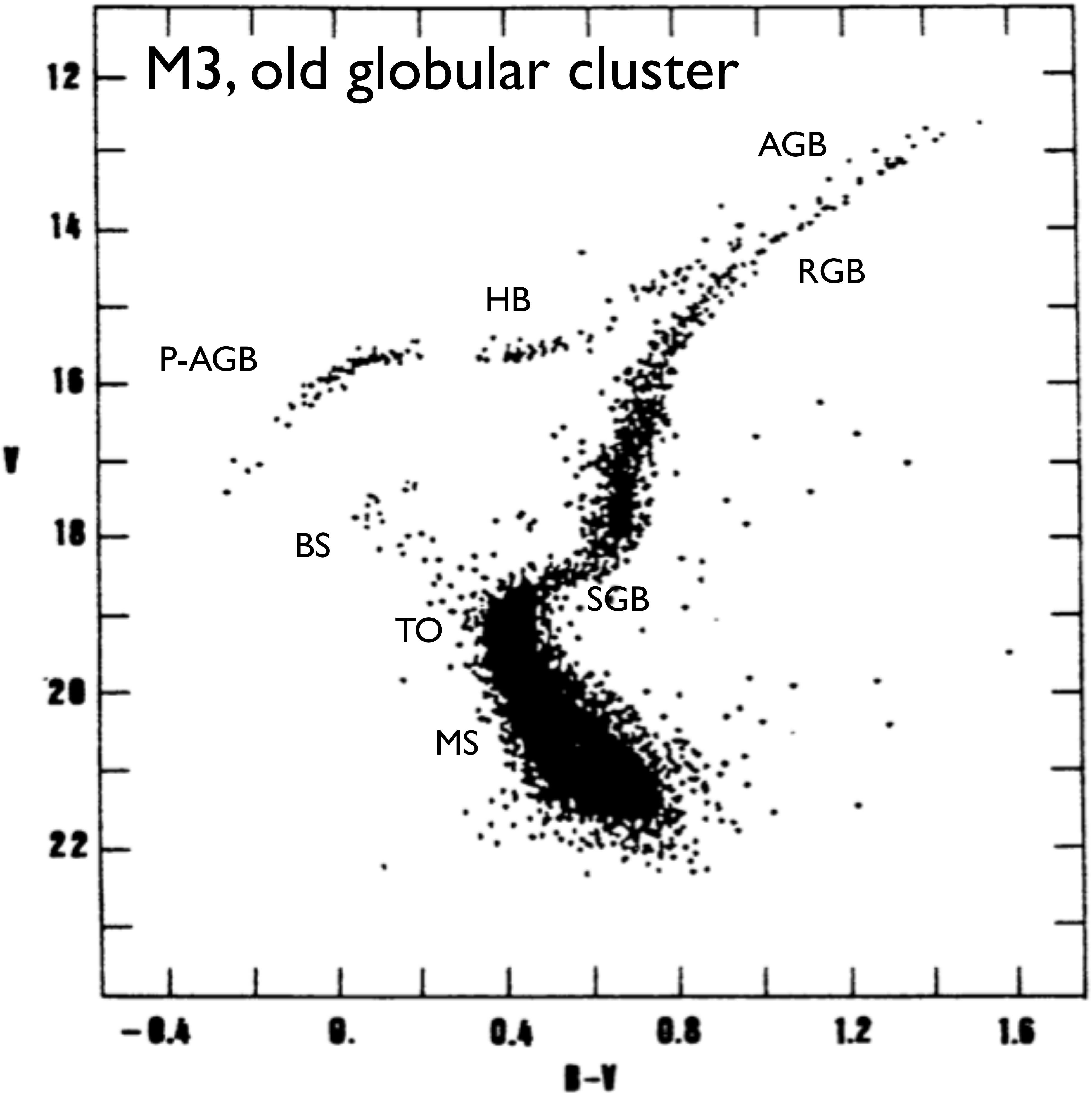
M3, old globular cluster
AGB
RGB
HB
P-AGB
BS
SGB
TO
MS
V
12
14
16
18
20
22
−0.4
0.
0.4
0.8
1.2
1.6
B−V

Table 6-2 Zero-age model for three compositions with $\mathfrak{M} = 2.82\mathfrak{M}_\odot$†

	X	Y	Z	$\frac{R}{R_\odot}$	$\frac{\mathfrak{L}}{\mathfrak{L}_\odot}$	$\log T_e$
Surface	0.60	0.36	0.04	2.1	93	4.10
	0.60	0.37	0.03	2.0	110	4.12
	0.70	0.27	0.03	2.0	63	4.07

$\frac{r}{R}$	X	Y	Z	$\frac{M(r)}{\mathfrak{M}}$	$\frac{L(r)}{\mathfrak{L}}$	$\log T$	$\log \rho$	κ
0.95	0.60	0.36	0.04	1.000	1.00	5.42	−4.81	7.6
	0.60	0.37	0.03	1.000	1.00	5.44	−4.74	7.0
	0.70	0.27	0.03	1.000	1.00	5.41	−4.73	8.9
0.85	0.60	0.36	0.04	1.000	1.00	5.92	−3.04	4.1
	0.60	0.37	0.03	1.000	1.00	5.94	−2.97	3.5
	0.70	0.27	0.03	1.000	1.00	5.91	−2.97	4.4
0.75	0.60	0.36	0.04	0.998	1.00	6.20	−2.09	3.8
	0.60	0.37	0.03	0.998	1.00	6.22	−2.02	3.3
	0.70	0.27	0.03	0.998	1.00	6.19	−2.02	4.0
0.65	0.60	0.36	0.04	0.992	1.00	6.43	−1.43	3.8
	0.60	0.37	0.03	0.992	1.00	6.44	−1.36	3.2
	0.70	0.27	0.03	0.992	1.00	6.42	−1.36	4.0
0.55	0.60	0.36	0.04	0.975	1.00	6.60	−0.85	2.78
	0.60	0.37	0.03	0.973	1.00	6.61	−0.77	2.31
	0.70	0.27	0.03	0.974	1.00	6.59	−0.77	2.90
0.45	0.60	0.36	0.04	0.926	1.00	6.75	−0.26	1.78
	0.60	0.37	0.03	0.922	1.00	6.76	−0.18	1.45
	0.70	0.27	0.03	0.925	1.00	6.74	−0.19	1.86
0.35	0.60	0.36	0.04	0.806	1.00	6.90	+0.34	1.20
	0.60	0.37	0.03	0.795	1.00	6.92	0.41	1.01
	0.70	0.27	0.03	0.804	1.00	6.89	0.41	1.25
0.25	0.60	0.36	0.04	0.546	1.00	7.06	0.91	0.80
	0.60	0.37	0.03	0.527	1.00	7.08	0.96	0.72
	0.70	0.27	0.03	0.544	1.00	7.05	0.98	0.84
0.20	0.60	0.36	0.04	0.365	1.00	7.15	1.14	0.66
	0.60	0.37	0.03	0.347	1.00	7.17	1.18	0.60
	0.70	0.27	0.03	0.362	0.99	7.14	1.21	0.71
0.15	0.60	0.36	0.04	0.190	0.98	7.24	1.32	0.56
	0.60	0.37	0.03	0.179	0.98	7.25	1.35	Conv.
	0.70	0.27	0.03	0.188	0.97	7.22	1.38	0.59
0.10	0.60	0.36	0.04	0.065	0.82	7.31	1.43	Conv.
	0.60	0.37	0.03	0.062	0.80	7.32	1.45	Conv.
	0.70	0.27	0.03	0.065	0.79	7.30	1.49	Conv.
0.05	0.60	0.36	0.04	0.010	0.26	7.35	1.49	Conv.
	0.60	0.37	0.03	0.008	0.24	7.36	1.51	Conv.
	0.70	0.27	0.03	0.009	0.25	7.34	1.56	Conv.

Table 6-2 Zero-age model for three compositions with $\mathfrak{M} = 2.82\mathfrak{M}_\odot$† (Continued)

	X	Y	Z	$\frac{R}{R_\odot}$	$\frac{\mathfrak{L}}{\mathfrak{L}_\odot}$	$\log T_e$
Surface	0.60	0.36	0.04	2.1	93	4.10
	0.60	0.37	0.03	2.0	110	4.12
	0.70	0.27	0.03	2.0	63	4.07

$\frac{r}{R}$	X	Y	Z	$\frac{M(r)}{\mathfrak{M}}$	$\frac{L(r)}{\mathfrak{L}}$	$\log T$	$\log \rho$	κ
0.00	0.60	0.36	0.04	0.000	0.00	7.36	1.51	Conv.
	0.60	0.37	0.03	0.000	0.00	7.37	1.53	Conv.
	0.70	0.27	0.03	0.000	0.00	7.35	1.58	Conv.
0.148‡	0.60	0.36	0.04	0.183	0.98	7.24	1.32	0.55
0.155‡	0.60	0.37	0.03	0.194	0.98	7.24	1.33	0.53
0.147‡	0.70	0.27	0.03	0.179	0.97	7.23	1.39	0.59

† Adapted from B. Strömgren, Stellar Models for Main-sequence Stars and Subdwarfs, in L. H. Aller and D. B. McLaughlin (eds.), "Stellar Structure." By permission of The University of Chicago Press. Copyright 1965 by The University of Chicago.

‡ Boundary of the convective core.

Table 6-3 Zero-age model for three compositions with $\mathfrak{M} = 7.08\mathfrak{M}_\odot$†

	X	Y	Z	$\frac{R}{R_\odot}$	$\frac{\mathfrak{L}}{\mathfrak{L}_\odot}$	$\log T_e$
Surface	0.60	0.36	0.04	3.5	2,800	4.35
	0.60	0.37	0.03	3.4	2,800	4.36
	0.70	0.27	0.03	3.3	2,000	4.35

$\frac{r}{R}$	X	Y	Z	$\frac{M(r)}{\mathfrak{M}}$	$\frac{L(r)}{\mathfrak{L}}$	$\log T$	$\log \rho$	κ
0.95	0.60	0.36	0.04	1.000	1.00	5.59	−4.77	1.88
	0.60	0.37	0.03	1.000	1.00	5.61	−4.70	1.72
	0.70	0.27	0.03	1.000	1.00	5.58	−4.72	2.09
0.85	0.60	0.36	0.04	1.000	1.00	6.09	−3.06	1.34
	0.60	0.37	0.03	1.000	1.00	6.10	−2.99	1.22
	0.70	0.27	0.03	1.000	1.00	6.08	−2.99	1.42
0.75	0.60	0.36	0.04	0.997	1.00	6.38	−2.18	1.33
	0.60	0.37	0.03	0.997	1.00	6.39	−2.10	1.19
	0.70	0.27	0.03	0.997	1.00	6.37	−2.10	1.43
0.65	0.60	0.36	0.04	0.987	1.00	6.59	−1.52	1.10
	0.60	0.37	0.03	0.987	1.00	6.60	−1.44	0.95
	0.70	0.27	0.03	0.987	1.00	6.58	−1.44	1.16
0.55	0.60	0.36	0.04	0.958	1.00	6.75	−0.92	0.81
	0.60	0.37	0.03	0.955	1.00	6.77	−0.85	0.70
	0.70	0.27	0.03	0.957	1.00	6.74	−0.85	0.87
0.45	0.60	0.36	0.04	0.880	1.00	6.91	−0.35	0.64
	0.60	0.37	0.03	0.872	1.00	6.93	−0.28	0.58
	0.70	0.27	0.03	0.878	1.00	6.90	−0.28	0.68
0.35	0.60	0.36	0.04	0.705	1.00	7.07	+0.18	0.50
	0.60	0.37	0.03	0.689	1.00	7.08	0.24	0.47
	0.70	0.27	0.03	0.702	1.00	7.06	0.25	0.53
0.25	0.60	0.36	0.04	0.410	1.00	7.23	0.61	0.41
	0.60	0.37	0.03	0.393	1.00	7.24	0.65	0.39
	0.70	0.27	0.03	0.407	1.00	7.22	0.67	0.44
0.20	0.60	0.36	0.04	0.252	1.00	7.31	0.75	Conv
	0.60	0.37	0.03	0.239	0.99	7.32	0.78	Conv.
	0.70	0.27	0.03	0.249	1.00	7.30	0.82	Conv
0.15	0.60	0.36	0.04	0.123	0.94	7.37	0.86	Conv
	0.60	0.37	0.03	0.116	0.93	7.38	0.89	Conv
	0.70	0.27	0.03	0.125	0.94	7.36	0.93	Conv
0.10	0.60	0.36	0.04	0.041	0.66	7.42	0.94	Conv
	0.60	0.37	0.03	0.038	0.64	7.43	0.96	Conv
	0.70	0.27	0.03	0.040	0.67	7.41	1.00	Conv
0.05	0.60	0.36	0.04	0.006	0.16	7.45	0.99	Conv
	0.60	0.37	0.03	0.005	0.11	7.45	1.01	Conv
	0.70	0.27	0.03	0.005	0.16	7.44	1.05	Conv

Table 6-3 Zero-age model for three compositions with $\mathfrak{M} = 7.08\mathfrak{M}_\odot$† (Continued)

	X	Y	Z	$\frac{R}{R_\odot}$	$\frac{\mathfrak{L}}{\mathfrak{L}_\odot}$	$\log T_e$
Surface	0.60	0.36	0.04	3.5	2,800	4.35
	0.60	0.37	0.03	3.4	2,800	4.36
	0.70	0.27	0.03	3.3	2,000	4.35

$\frac{r}{R}$	X	Y	Z	$\frac{M(r)}{\mathfrak{M}}$	$\frac{L(r)}{\mathfrak{L}}$	$\log T$	$\log \rho$	κ
0.00	0.60	0.36	0.04	0.000	0.00	7.45	1.00	Conv.
	0.60	0.37	0.03	0.000	0.00	7.46	1.02	Conv.
	0.70	0.27	0.03	0.000	0.00	7.45	1.06	Conv.
0.211‡	0.60	0.36	0.04	0.282	1.00	7.29	0.73	0.39
0.218‡	0.60	0.37	0.03	0.290	1.00	7.30	0.74	0.38
0.207‡	0.70	0.27	0.03	0.270	1.00	7.29	0.80	0.42

† Adapted from B. Strömgren, Stellar Models for Main-sequence Stars and Subdwarfs, in L. H. Aller and D. B. McLaughlin (eds.), "Stellar Structure." By permission of The University of Chicago Press. Copyright 1965 by The University of Chicago.

‡ Boundary of the convective core.

Table 6-4 Evolved main sequence for four masses†

$\mathfrak{M}/\mathfrak{M}_\odot$	X_c	*Age,* 10^6 *years*	$R/R_\odot$	M_b	$\log T_e$	$\lvert\Delta M_b\rvert$	$q(core)$	T_c, 10^6 °K	ρ_c, g/cm^3
1.78	0.70	0	1.54	2.1	3.93	0.0	0.12	20	68
	0.60	210	1.64	2.0	3.92	0.1	0.11	20	72
	0.50	390	1.74	2.0	3.92	0.3	0.10	21	76
	0.40	540	1.86	2.0	3.90	0.5	0.09	21	82
	0.30	670	1.99	1.9	3.89	0.7	0.08	22	89
	0.20	770	2.14	1.9	3.88	0.9	0.07	22	99
	0.10	860	2.28	1.9	3.86	1.0	0.06	24	117
2.82	0.70	0	1.96	0.2	4.07	0.0	0.18	23	38
	0.60	70	2.11	0.1	4.07	0.2	0.16	23	39
	0.50	120	2.28	0.0	4.06	0.4	0.14	24	41
	0.40	170	2.46	−0.1	4.05	0.6	0.12	24	43
	0.30	210	2.67	−0.1	4.03	0.8	0.10	25	46
	0.20	240	2.91	−0.1	4.02	1.1	0.08	25	50
	0.10	260	3.15	−0.1	4.00	1.3	0.07	27	59
4.47	0.70	0	2.54	−1.7	4.20	0.0	0.22	25	21
	0.60	23	2.75	−1.8	4.20	0.2	0.20	26	21
	0.50	42	2.99	−1.9	4.19	0.4	0.17	26	22
	0.40	56	3.26	−2.0	4.18	0.7	0.15	27	22
	0.30	68	3.57	−2.0	4.16	0.9	0.12	28	24
	0.20	78	3.91	−2.1	4.15	1.2	0.10	28	26
	0.10	86	4.27	−2.1	4.13	1.5	0.08	30	30
7.08	0.70	0	3.3	−3.5	4.32	0.0	0.27	28	12
	0.60	9	3.6	−3.6	4.32	0.2	0.24	29	12
	0.50	16	3.9	−3.7	4.31	0.4	0.21	29	12
	0.40	21	4.3	−3.8	4.30	0.7	0.18	30	12
	0.30	26	4.7	−3.9	4.29	1.0	0.16	31	13
	0.20	29	5.2	−3.9	4.27	1.3	0.13	32	14
	0.10	32	5.8	−4.0	4.26	1.5	0.11	33	16

† Adapted from B. Strömgren, Stellar Models for Main-sequence Stars and Subdwarfs, in L. H. Aller and D. B. McLaughlin (eds.), "Stellar Structure." By permission of The University of Chicago Press. Copyright 1965 by The University of Chicago. The initial composition is $X = 0.70$, $Y = 0.27$, $Z = 0.03$.

Table 6-5 Zero-age model of the sun†

$M(r)$, solar masses	r, 10^{11} cm	T, 10^6 °K	ρ, g/cm³	$L(r)$, 10^{33} ergs/sec	ϵ, ergs g^{-1} sec^{-1}	κ, cm²/g
0.0	0.00	13.7	90	0.00	13.9	1.38
0.05	0.07	12.3	74	0.95	7.2	1.64
0.1	0.09	11.6	65	1.54	4.8	1.82
0.2	0.11	10.4	51	2.20	2.3	2.16
0.3	0.14	9.4	40	2.53	1.1	2.50
0.4	0.16	8.5	30.5	2.68	0.5	2.87
0.5	0.18	7.6	22.4	2.75	0.2	3.3
0.6	0.20	6.8	15.7	2.77	0.04	3.8
0.7	0.23	5.9	10.0	2.78	0.01	4.4
0.8	0.26	5.0	5.5	2.78	0.00	5.2
0.9	0.32	3.8	2.09	2.78	0.00	7.0
0.95	0.37	3.0	0.87	2.78	0.00	8.6
0.99	0.46	1.73	0.142	2.78	0.00	11.1
0.99968	0.60	0.62	0.0057	2.78	0.00	Conv.
1.0	0.659			2.78		

† B. Strömgren, Stellar Models for Main-sequence Stars and Subdwarfs, in L. H. Aller and D. B. McLaughlin (eds.), "Stellar Structure." By permission of The University of Chicago Press. Copyright 1965 by The University of Chicago.

Table 6-6 Model of the sun at 4.5 × 10⁹ years†

$M(r)$, solar masses	r, 10^{11} cm	T, 10^6 °K	ρ, g/cm³	$L(r)$, 10^{33} ergs/sec	ϵ, ergs g^{-1} sec^{-1}	κ, cm²/g	X_H
0.0	0.00	15.7	158	0.00	17.5	1.09	0.36
0.05	0.06	13.8	103	1.30	10.0	1.32	0.52
0.1	0.08	12.8	83	2.13	6.8	1.48	0.58
0.2	0.10	11.3	59	3.09	3.3	1.78	0.65
0.3	0.13	10.1	43	3.55	1.6	2.09	0.68
0.4	0.15	9.0	31.5	3.77	0.7	2.42	0.69
0.5	0.17	8.1	22.4	3.86	0.3	2.79	0.70
0.6	0.20	7.1	15.2	3.90	0.06	3.2	0.70
0.7	0.23	6.2	9.4	3.90	0.02	3.8	0.71
0.8	0.26	5.1	5.0	3.90	0.00	4.5	0.71
0.9	0.32	3.9	1.84	3.90	0.00	6.0	0.71
0.95	0.38	3.0	0.74	3.90	0.00	7.4	0.71
0.99	0.48	1.73	0.117	3.90	0.00	9.6	0.71
0.99955	0.62	0.66	0.0063	3.90	0.00	Conv.	0.71
1.0	0.694			3.90			0.71

† B. Strömgren, Stellar Models for Main-sequence Stars and Subdwarfs, in L. H. Aller and D. B. McLaughlin (eds.), "Stellar Structure." By permission of The University of Chicago Press. Copyright 1965 by The University of Chicago. Initial composition $X = 0.71$, $Y = 0.27$.

Table 6-7 Evolutionary lifetime for $3\mathfrak{M}_\odot$†

Point	t, 10^8 years	Point	t, 10^8 years	Point	t, 10^8 years
1	0.024586	7	2.47004	14	2.55850
2	1.38921	8	2.47865	15	2.78295
3	2.23669	9	2.48429	16	2.94233
4	2.34089	10	2.48925	17	3.06968
4′	2.34222	11	2.49817	18	3.19043
5	2.40119	12	2.50728	19	3.23566
6	2.44420	13	2.53163	20	3.26323

† I. Iben, Jr., *Astrophys. J.*, **142**:1447 (1965). By permission of The University of Chicago Press. Copyright 1965 by The University of Chicago.

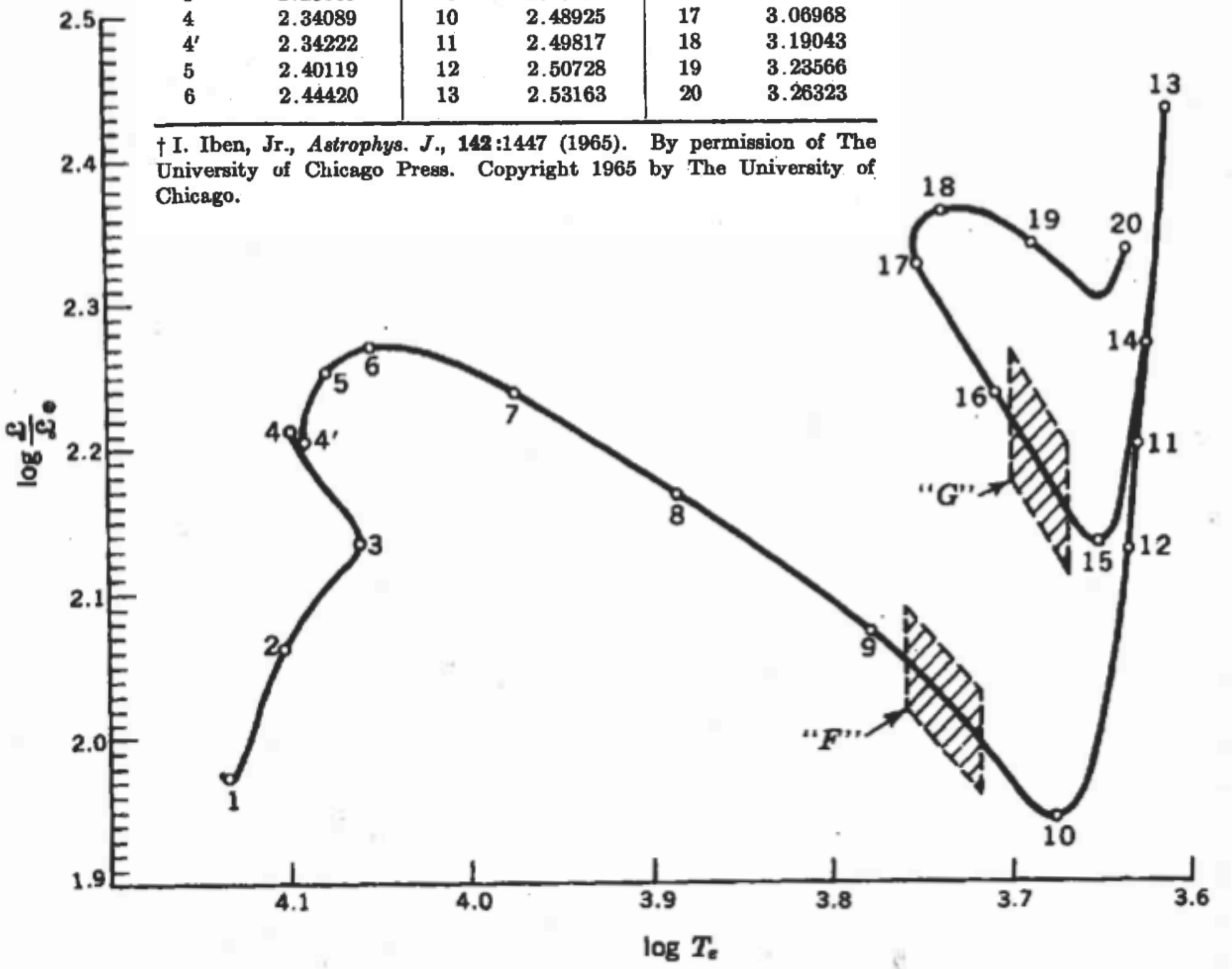

Fig. 6-13 The evolutionary track of a star of three solar masses in the H-R diagram. The time required to reach the enumerated points is given in Table 6-7. [*After I. Iben, Jr., Astrophys. J.*, **142**:1447 (1965). *By permission of The University of Chicago Press. Copyright* 1965 *by The University of Chicago.*]

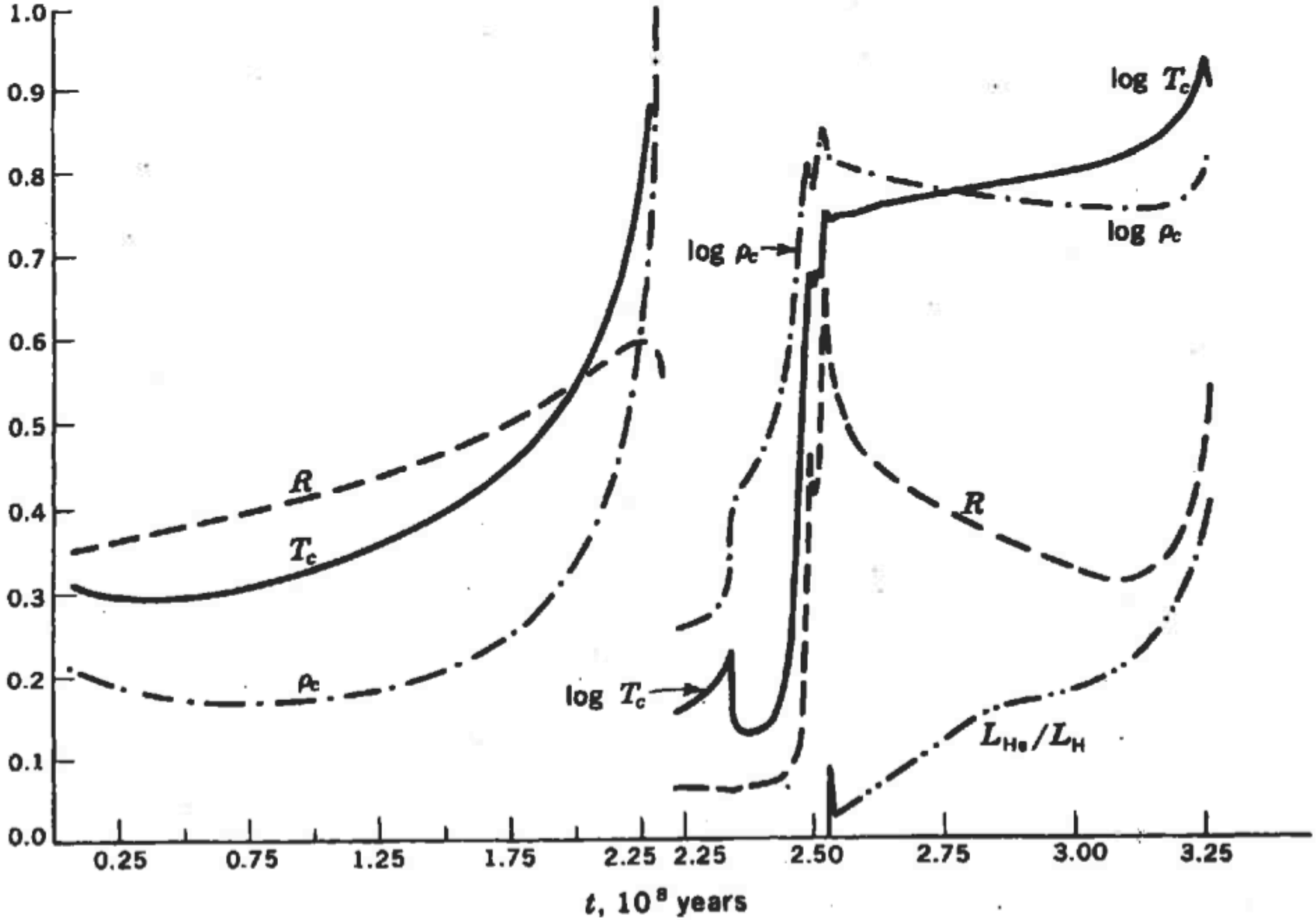

Fig. 6-15 The variation with time of the radius, the central density, the central temperature, and the ratio of the helium-burning power to the hydrogen-burning power during the evolution of a three-solar-mass star. To the left of the break at $t = 2.25 \times 10^8$ years the full-scale limits correspond to $5 > R/R_\odot > 0$, $31 > T_c/10^6 > 21$, and $80 > \rho_c > 30$. To the right of the break the full-scale limits correspond to $50 > R/R_\odot > 0$, $2.3 > \log T_c/10^6 > 1.3$, $5.5 > \log \rho_c > 0.5$, and $1.0 > L_{He}/L_H > 0$. [*After I. Iben, Jr., Astrophys. J.*, **142**:1447 (1965). *By permission of The University of Chicago Press. Copyright* 1965 *by The University of Chicago.*]

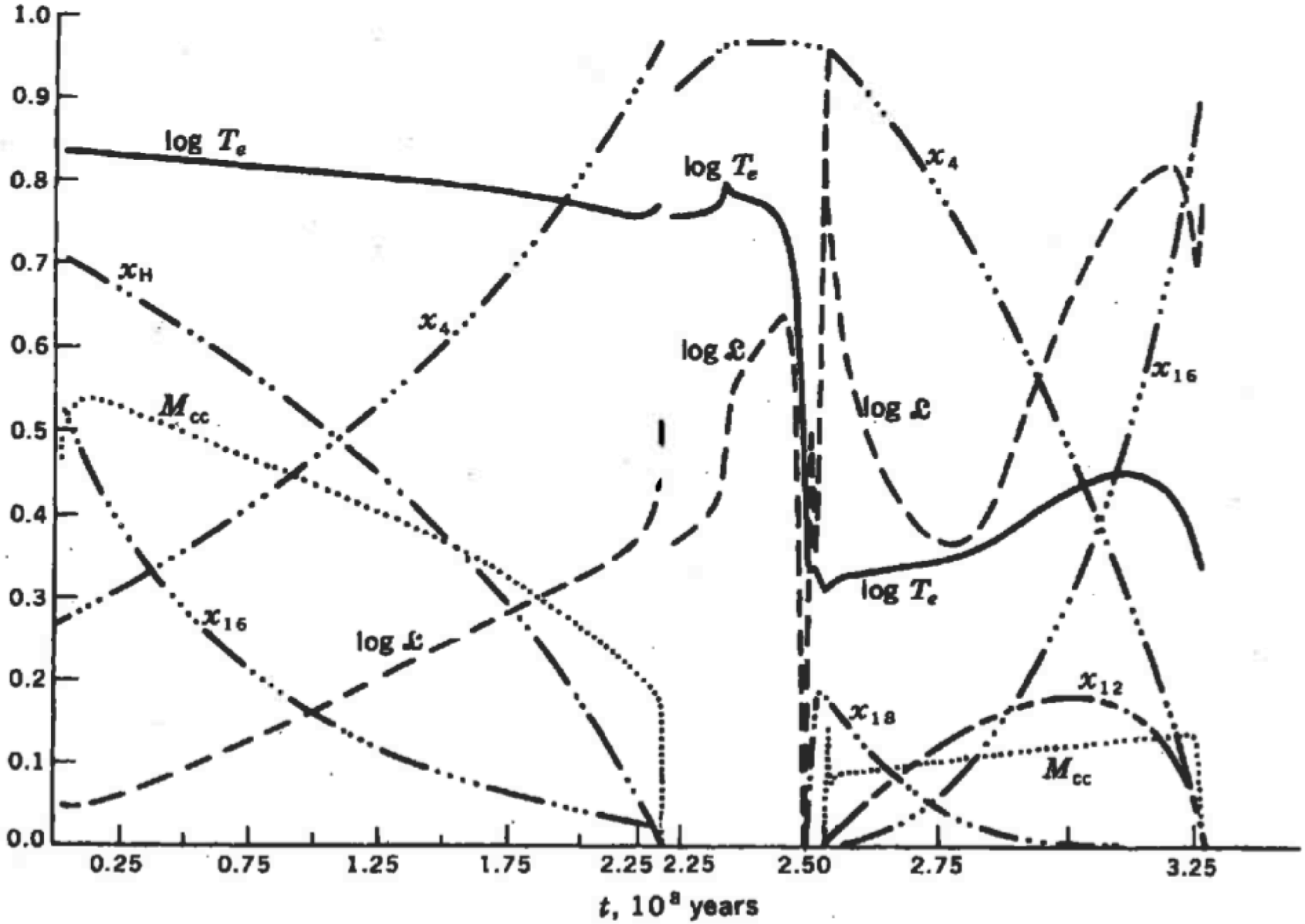

Fig. 6-14 The variation with time of the luminosity, the surface temperature, the mass fraction M_{cc} within the convective core, and the central mass fractions of H, He^4, C^{12}, O^{16}, and O^{18} during the evolution of a three-solar-mass star. The full-scale limits correspond to $2.45 > \log \mathfrak{L}/\mathfrak{L}_\odot > 1.95$, $4.3 > \log T_e > 3.3$, and $\frac{1}{3} > M_{cc} > 0$. The scale for the composition parameters changes at $t = 2.25 \times 10^8$ years. To the left of the break $0.02 > X_{16} > 0$ and $1.0 > x_H, X_4 > 0$, and to the right of the break $0.1 > X_{18} > 0$ and $1.0 > X_4, X_{12}, X_{16} > 0$. [*After I. Iben, Jr., Astrophys. J.*, **142**:1447 (1965). *By permission of The University of Chicago Press. Copyright* 1965 *by The University of Chicago.*]

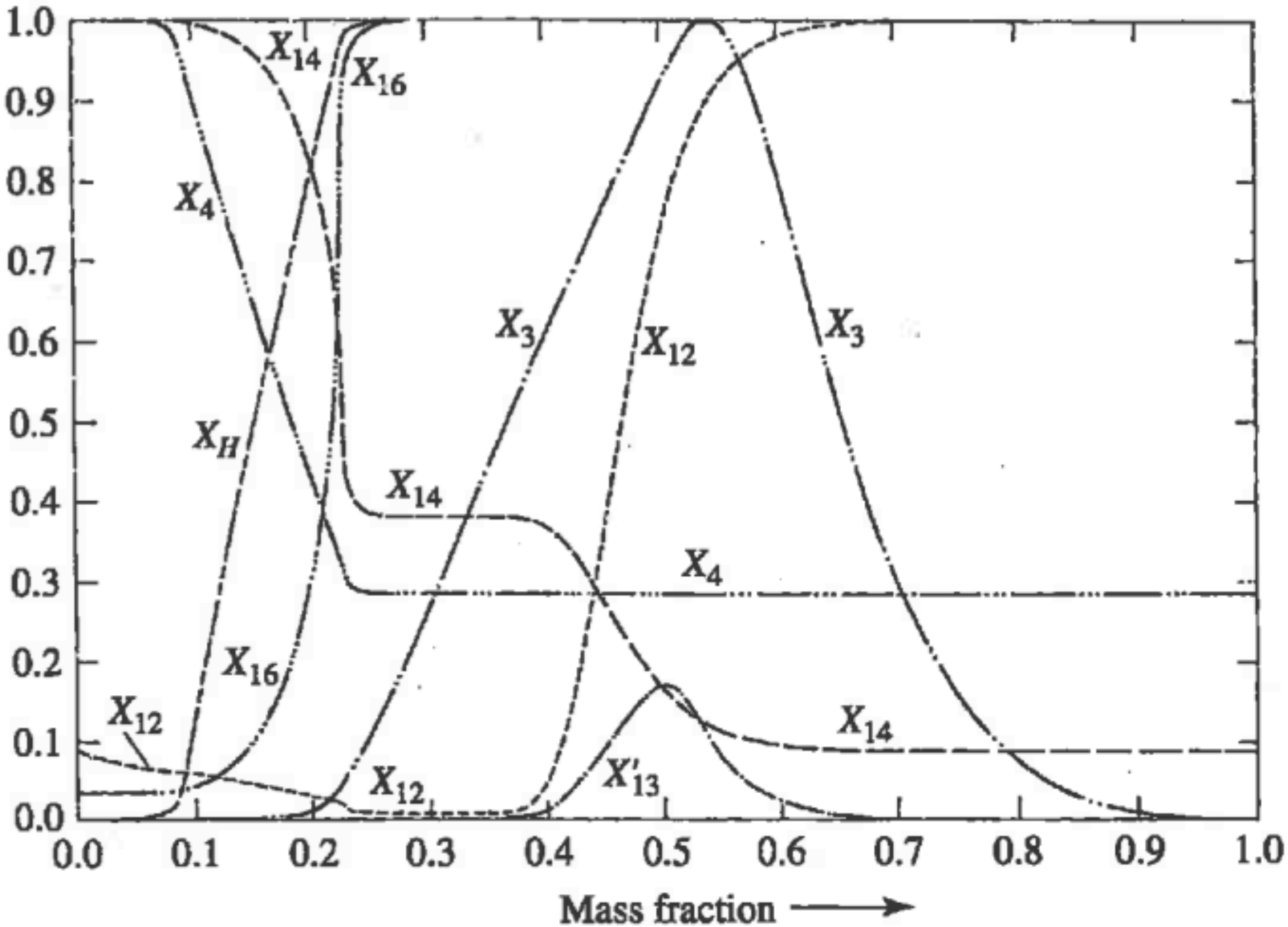

FIGURE 13.6 The chemical composition as a function of interior mass fraction for a 5 $M_\odot$ star during the phase of overall contraction, following the main-sequence phase of core hydrogen burning. The maximum mass fractions of the indicated species are $X_H = 0.708$, $X_3 = 1.296 \times 10^{-4}$ ($^3_2$He), $X_4 = 0.9762$ ($^4_2$He), $X_{12} = 3.61 \times 10^{-3}$ ($^{12}_6$C), $X'_{13} = 3.61 \times 10^{-3}$ ($^{13}_6$C), $X_{14} = 0.0145$ ($^{14}_7$N), and $X_{16} = 0.01080$ ($^{16}_8$O). (Figure adapted from Iben, *Ap. J.*, *143*, 483, 1966.)

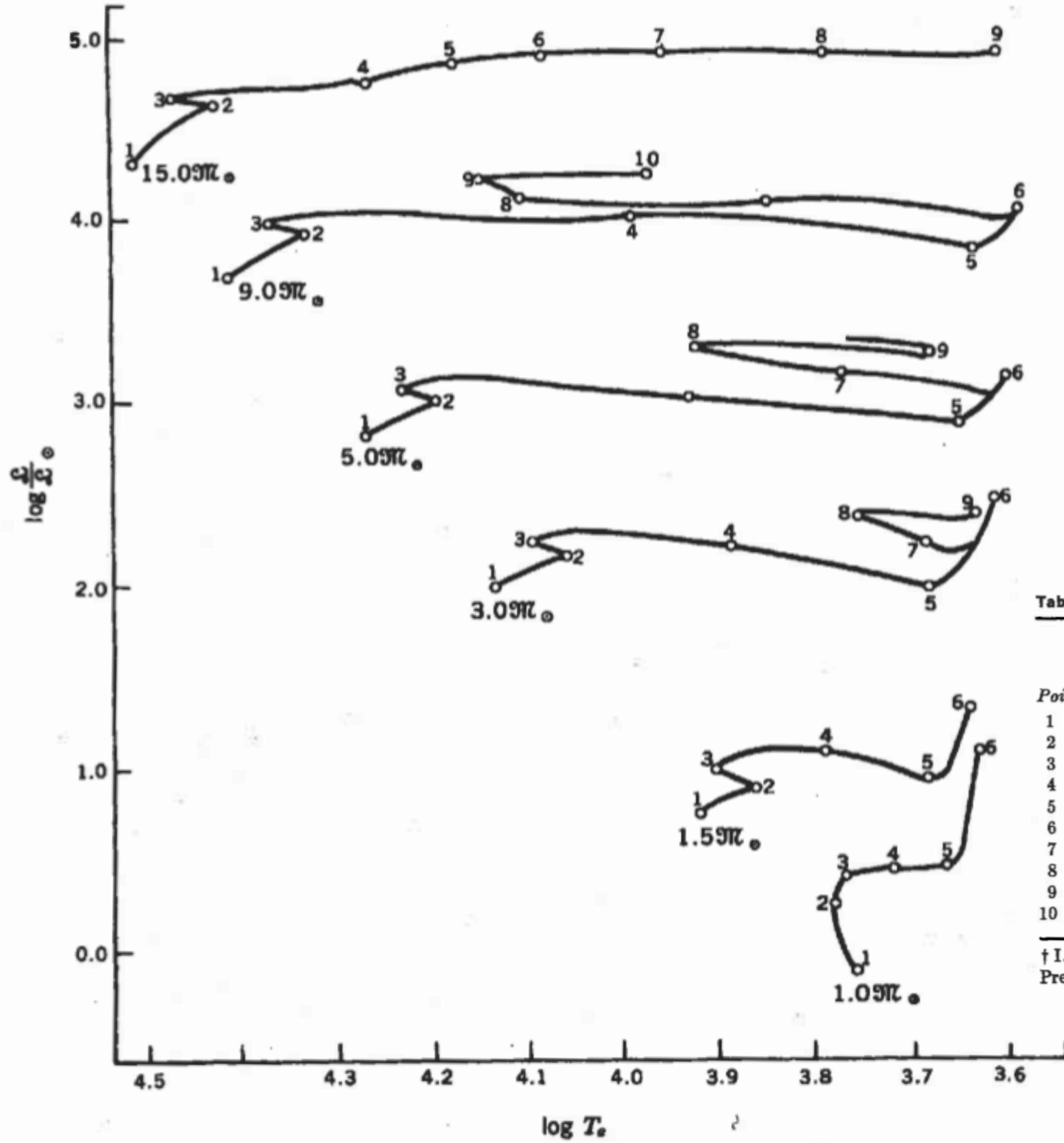

Fig. 6-16 Evolutionary paths in the H-R diagram for population I stars of mass $\mathfrak{M}/\mathfrak{M}_\odot$ = 1.0, 1.5, 3, 5, 9, and 15. The initial point is on the zero-age main sequence. The ages of the stars at the enumerated points are listed in Table 6-8. [*After I. Iben, Jr., Astrophys. J.*, **140**:1631 (1964). *By permission of The University of Chicago Press. Copyright* 1964 *by The University of Chicago.*]

Table 6-8 Evolutionary lifetimes, years†

	$\mathfrak{M}/\mathfrak{M}_\odot$					
Point	15.0	9.0	5.0	3.0	1.5	1.0
1	6.160×10^4	1.511×10^5	5.760×10^5	2.510×10^6	1.821×10^7	5.016×10^7
2	1.023×10^7	2.129×10^7	6.549×10^7	2.273×10^8	1.567×10^9	8.060×10^9
3	1.048×10^7	2.190×10^7	6.823×10^7	2.394×10^8	1.652×10^9	9.705×10^9
4	1.050×10^7	2.208×10^7	7.019×10^7	2.478×10^8	2.036×10^9	1.0236×10^{10}
5	1.149×10^7	2.213×10^7	7.035×10^7	2.488×10^8	2.105×10^9	1.0446×10^{10}
6	1.196×10^7	2.214×10^7	7.084×10^7	2.531×10^8	2.263×10^9	1.0875×10^{10}
7	1.210×10^7	2.273×10^7	7.844×10^7	2.887×10^8		
8	1.213×10^7	2.315×10^7	8.524×10^7	3.095×10^8		
9	1.214×10^7	2.574×10^7	8.782×10^7	3.262×10^8		
10		2.623×10^7				

† I. Iben, Jr., *Astrophys. J.*, **140**:1631 (1964). By permission of The University of Chicago Press. Copyright 1964 by The University of Chicago.

Table 6.9 Evolutionary lifetimes (10^9 years)†

Point	$1.0\mathfrak{M}_\odot$	$1.25\mathfrak{M}_\odot$	$1.50\mathfrak{M}_\odot$
1	0.05060	0.02954	0.01821
2	3.8209	1.4220	1.0277
3	6.7100	2.8320	1.5710
4	8.1719	3.0144	1.6520
5	9.2012	3.5524	1.8261
6	9.9030	3.9213	1.9666
7	10.195	4.0597	2.0010
8		4.1204	2.0397
9		4.1593	2.0676
10	10.352	4.2060	2.1059
11	10.565	4.3427	2.1991
12	10.750	4.4505	2.2628
13	10.875	4.5349	

† I. Iben, Jr., *Astrophys. J.*, **147**:624 (1967). By permission of The University of Chicago Press. Copyright 1967 by The University of Chicago.

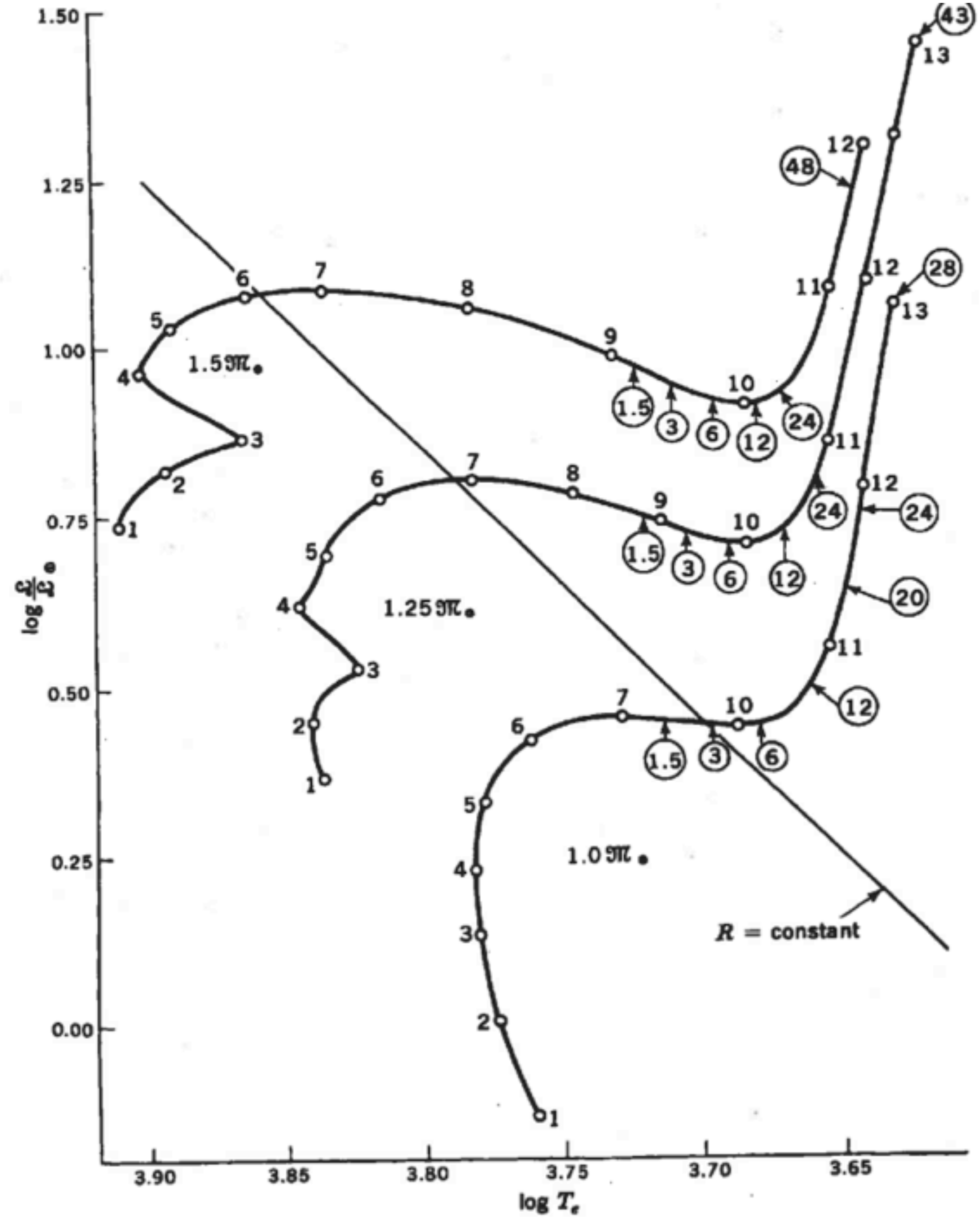

Fig. 6-17 Evolutionary track of lower-main-sequence population I stars of mass $\mathfrak{M}/\mathfrak{M}_\odot = 1.0$, 1.25, and 1.5. The ages of the stars at the enumerated points along each track are listed in Table 6-9. The circled numbers along the tracks represent the factors by which the surface Li^7 abundance has been depleted by the deepening of the outer convection zone. A diagonal line of constant radius has been included for added physical insight. [*After I. Iben, Jr., Astrophys. J.*, **147**:624 (1967). *By permission of The University of Chicago Press. Copyright* 1967 *by The University of Chicago.*]

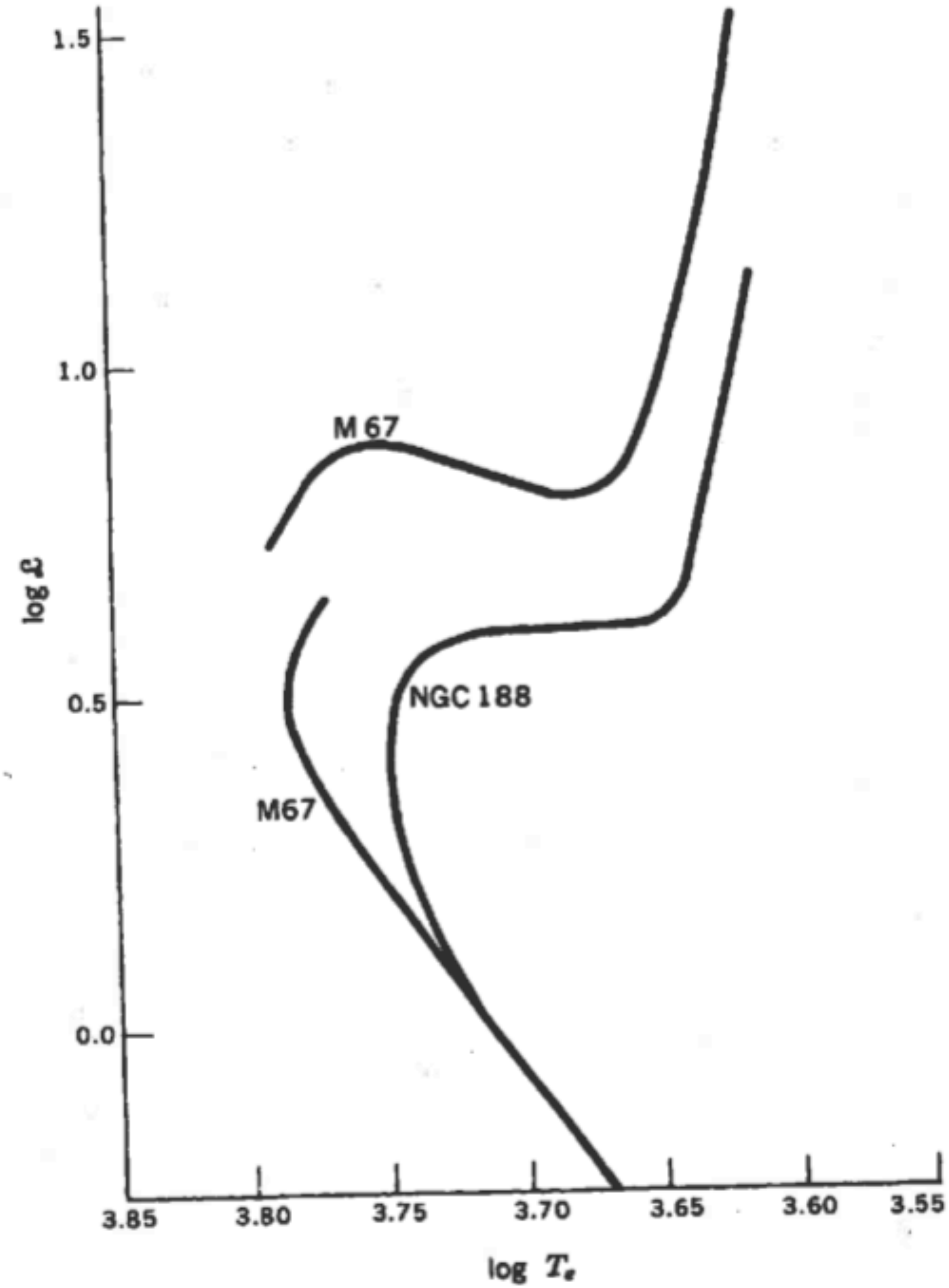

Fig. 6-18 A characterization of the observed H-R diagrams of two old galactic clusters. The ages of these clusters are estimated by the age of an ensemble of stellar models having the property that the locus of H-R positions of the individual stars within the ensemble, which differ with respect to mass only, best reproduces the observed diagram of the cluster. [*After I. Iben, Jr., Astrophys. J.*, **147**:624 (1967). *By permission of The University of Chicago Press. Copyright* 1967 *by The University of Chicago.*]